Ore Geology Reviews 90 (2017) 465–484

Contents lists available at ScienceDirect

Ore Geology Reviews

journal homepage: www.elsevier.com/locate/oregeorev

Roles of xenomelts, xenoliths, xenocrysts, xenovolatiles, residues, and skarns in the genesis, transport, and localization of magmatic Fe-Ni-Cu-PGE sulfides and chromite

C.M. Lesher

Mineral Exploration Research Centre, Harquail School of Earth Sciences and Goodman School of Mines, Laurentian University, Sudbury, Ontario P3E 2C6, Canada

ARTICLE INFO

Keywords:
Xenoliths
Xenomelts
Sulfide transport
Ore localization
Fe-Ni-Cu-PGE
Sulfide
Chromite

ABSTRACT

Most sulfide-rich magmatic Ni-Cu-(PGE) deposits form in dynamic magmatic systems by partial melting S-bearing wall rocks with variable degrees of assimilation of miscible silicate and volatile components, and generation of barren to weakly-mineralized immiscible Fe sulfide xenomelts into which Ni-Cu-Co-PGE partition from the magma. Some exceptionally-thick magmatic Cr deposits may form by partial melting oxide-bearing wall rocks with variable degrees of assimilation of the miscible silicate and volatile components, and generation of barren Fe ± Ti oxide xenocrysts into which Cr-Mg-V ± Ti partition from the magma. The products of these processes are variably preserved as skarns, residues, xenoliths, xenocrysts, xenomelts, and xenovolatiles, which play important to critical roles in ore genesis, transport, localization, and/or modification. Incorporation of barren xenoliths/autoliths may induce small amounts of sulfide/chromite to segregate, but incorporation of sulfide xenomelts or oxide xenocrysts with dynamic upgrading of metal tenors (PGE > Cu > Ni > Co and Cr > V > Ti, respectively) is required to make significant ore deposits. Silicate xenomelts are only rarely preserved, but will be variably depleted in chalcophile and ferrous metals. Less dense felsic xenoliths may aid upward sulfide transport by increasing the effective viscosity and decreasing the bulk density of the magma. Denser mafic or metamorphosed xenoliths may also increase the effective viscosity of the magma, but may aid downward sulfide transport by increasing the bulk density of the magma. Sulfide wets olivine, so olivine xenocrysts may act as filter beds to collect advected finely dispersed sulfide droplets, but other silicates and xenoliths may not be wetted by sulfides. Xenovolatiles may retard settling of – or in some cases float – dense sulfide droplets. Reactions of sulfide melts with felsic country rocks may generate Fe-rich skarns that may allow sulfide melts to fractionate to more extreme Cu-Ni-rich compositions. Xenoliths, xenocrysts, xenomelts, and xenovolatiles are more likely to be preserved in cooler basaltic magmas than in hotter komatiitic magmas, and are more likely to be preserved in less dynamic (less turbulent) systems/domain/phases than in more dynamic (more turbulent) systems/domains/phases. Massive to semi-massive Ni-Cu-PGE and Cr mineralization and xenoliths are often localized within footwall embayments, dilations/jogs in dikes, throats of magma conduits, and the horizontal segments of dike-chonolith and dike-sill complexes, which represent fluid dynamic traps for both ascending and descending sulfides/oxides. If skarns, residues, xenoliths, xenocrysts, xenomelts, and/or xenovolatiles are present, they provide important constraints on ore genesis and they are valuable exploration indicators, but they must be included in elemental and isotopic mass balance calculations.

1. Introduction

Geological, geochemical, isotopic, thermodynamic, and fluid dynamic constraints require that the sulfide in most high-grade magmatic Ni-Cu-(PGE) deposits (e.g., Kambalda, Noril'sk, Pechenga, Raglan, Sudbury, Thompson, Voisey's Bay) was derived by melting of S-bearing country rocks during lava/magma emplacement (e.g., Lesher et al., 1984; Lesher and Groves, 1986; Ripley, 1986; Naldrett, 2004; Arndt et al., 2005; Barnes and Lightfoot, 2005; Keays and Lightfoot, 2010; Ripley and Li, 2013; Barnes et al., 2016). Because the solubility of sulfide in silicate melts is so low (e.g., Haughton et al., 1974; Shima and Naldrett, 1975; Wendlandt, 1982; Mavrogenes and O'Neill, 1999), any more than small amounts of sulfide must have existed as initially Co-Ni-Cu-PGE-poor sulfide xenomelts[1] that were upgraded through

E-mail address: mlesher@laurentian.ca.

[1] Xenomelts, xenocrysts, and xenovolatiles are foreign melts, crystals, and volatiles derived by partial or wholesale melting of country rocks or country-rock xenoliths. They are collectively referred to as xenophases.

http://dx.doi.org/10.1016/j.oregeorev.2017.08.008
Received 19 January 2017; Received in revised form 1 August 2017; Accepted 2 August 2017
Available online 07 August 2017

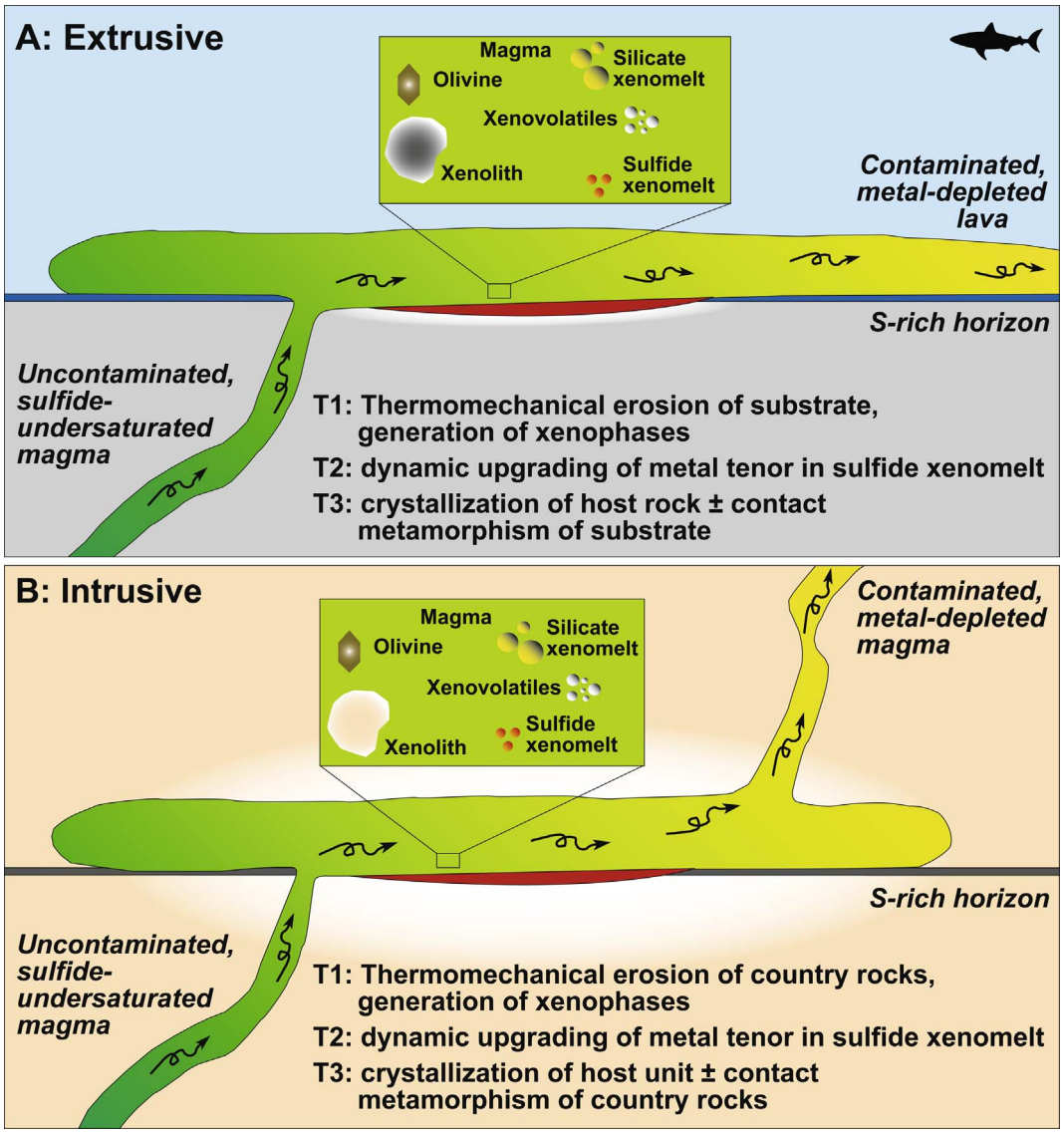

Fig. 1. Schematic models for dynamic (flow-through) volcanic (A) and subvolcanic/intrusive (B) systems involving early (**T1**) thermomechanical erosion of S-rich horizons and generation of xenoliths, sulfide xenomelts, silicate xenomelts, and xenovolatiles, followed by (**T2**) dynamic upgrading of metal tenors in sulfide xenomelts, and (**T3**) crystallization of the host unit with or without (depending on size and temperature of host unit and thermal state and physical properties) contact metamorphism of the substrate or country rocks. Modified after Lesher and Keays (2002).

interaction with the magma during transport and emplacement (Lesher and Campbell, 1993).

Similar arguments can be made that the oxide in some exceptionally-thick chromite deposits (e.g., Black Thor-Blackbird, possibly also Inyala, Ipueira-Medrado, Kemi, Nkomati, or Sukinda) may have been derived by partial melting of oxide-bearing country rocks during lava/magma emplacement. Because the solubility of Cr-rich spinel in most silicate melts is so low, it also would have existed as initially Cr-poor Fe ± Ti oxide xenocrysts that were converted to chromite through interaction with the magma during transport and emplacement (e.g., Lesher et al., 2014, 2016, submitted; Carson et al., 2015).

Despite the broad consensus on the need for external S to generate high-grade Ni-Cu-PGE deposits and emerging recognition of the need for external oxide to generate high-grade Cr deposits, there remain significant uncertainties regarding from where, in which direction, and how far sulfides/oxides were transported. Many models involve formation at depth with vertical transport to higher levels, but there are several problems with such models:

1) Fe-Cr oxides (up to 5.2 g cm^{-3}) and Fe-Ni-Cu sulfide melts (~4.2 g-cm^{-3}) are much denser than most silicate magmas (2.6–2.8 g-cm^{-3}) and most crustal rocks (2.7–2.9 g-cm^{-3}), which restricts the amounts of sulfide/oxide that can be transported in buoyantly rising magmas.
2) Xenoliths may reduce the effective viscosity and bulk density of the magma enough to allow the magma to transport greater amounts of sulfides, but the xenoliths in many systems are as dense or denser than the magma – either originally or after thermal metamorphism – and where well characterized (e.g., Duluth, Noril'sk, Voisey's Bay) they appear to be local country rocks, not deeper crustal rocks. Exceptions include Aguablanca and Sudbury, which contains exotic ultramafic inclusions not in equilibrium with the host magmas or present in the footwall/country rocks (e.g., Piña et al., 2006; Naldrett et al., 1984; Prevec et al., 2000)
3) Importantly, no Ni-Cu-PGE or Cr deposits are known to occur in lavas except where there is geological, stratigraphic, geochemical, and isotopic evidence that the sulfides formed at the same stratigraphic level (e.g., Alexo, Kambalda, Raglan), even when the subvolcanic plumbing systems locally contain significant mineralization

(e.g., Deccan, Duluth, Emeishan, Noril'sk, Thompson). Similarly, where there is subvolcanic mineralization, overlying lavas are not enriched in PGE, as would be expected from lavas carrying fine suspended sulfides even if S had been lost during degassing (S.J. Barnes, pers. comm., 2017).

Together, these points suggest that sulfides and oxides are not easily transported upwards and that the systems where we find them were very efficient in collecting these phases.

The aim of this paper is to discuss the roles of sulfide and silicate xenomelts, xenoliths, xenocrysts, xenovolatiles, residues, and skarns in the genesis of magmatic Ni-Cu-PGE deposits, but there are also implications for magmatic Cr deposits. As we shall see, these components not only influence the mass balance of metals in the ore-forming system, but they can play active roles in the formation, transport, and deposition of Fe-Ni-Cu-(PGE) sulfide melts and chromite.

2. Multi-component systems

Most geological, geochemical, and isotopic models for the formation of magmatic Ni-Cu-(PGE) and Cr deposits consider the system to contain only two or possibly three components: 1) a silicate magma and 2) an immiscible Fe-Ni-Cu-(PGE) sulfide melt or a crystalline Fe-Cr-(Mg)-(Al) oxide phase, with or without 3) olivine phenocrysts. In some cases, the systems are that simple, but in many cases, including the world-class Duluth, Kambalda, Noril'sk-Talnakh, Sudbury, and Voisey's Bay systems, they are more complex involving silicate magma, sulfide melt, xenoliths, silicate/oxide xenocrysts, silicate xenomelts, xenovolatiles, residues, and/or skarns (Fig. 1).

At Kambalda (Fig. 2), for example, the ore-forming system included a thick basaltic substrate covered by a thin cherty-sulfidic-graphitic sediment (Fig. 3B: unconsolidated at the time) that was covered by a channelized komatiite sheet flow containing multiple subparallel thicker higher-flux channel-flow facies flanked by multiple thinner lower-flux sheet-flow facies. The channel-flow facies were localized in topographic embayments, which have been *locally* modified by thermomechanical erosion along their bases and margins (e.g., Lesher et al., 1984; Groves et al., 1986; Frost and Groves, 1989a,b; Evans et al., 1989; Lesher, 1989; Staude et al., 2016, 2017). Overlying channelized sheet flows followed the same pitchlines and have eroded interflow sediments and the upper parts of the basal lava channel (Fig. 3A; Groves et al., 1986).

Because of the high temperature (~1640 °C) and low-viscosity (~0.1 Pa s^{-1}) of the komatiitic magma, in this case few xenoliths were preserved. Although channel- and sheet-flow facies contain abundant olivine, it crystallized after ore formation (Lesher, 1989). Silicate xenomelts are rare, but sedimentary xenomelts are locally preserved in the sheet-flow facies (Fig. 3C; Frost and Groves, 1989b) and basalt xenomelts are locally preserved within semi-massive sulfides along the base and margins of the embayments (Frost and Groves, 1989a; Staude et al., 2016, 2017). Residues of partially devolatilized sediments occur along the outside flanking margins of the ore-localizing embayments (Fig. 3D; Lesher and Burnham, 2001).

Each of these components is evident in the geochemical data (Fig. 4) where the components derived from the sediments (sulfide xenomelt, silicate xenomelt, and residues) define an extract triangle containing the bulk compositions of unmodified sediments). Exchange of metals between the lava and the sulfide xenomelts (e.g., Campbell and Naldrett, 1979; Lesher and Burnham, 2001) increased the metal contents of the sulfides (represented by the ores) and decreased the metal contents in the magmas (flushed downstream but rarely preserved as silicate xenomelts in the upper parts of the flanking sheet flows (Fig. 4; Lesher et al., 2001; Barnes et al., 2013).

The following sections will focus on each of the xenophases.

3. Sulfide xenomelts

The strongest evidence that some and in many cases most of the S in magmatic Ni-Cu-PGE deposits is derived from crustal rocks and not mantle-derived magmas is provided by S isotopic data (Fig. 5). Several points must be remembered when evaluating S isotopic data:

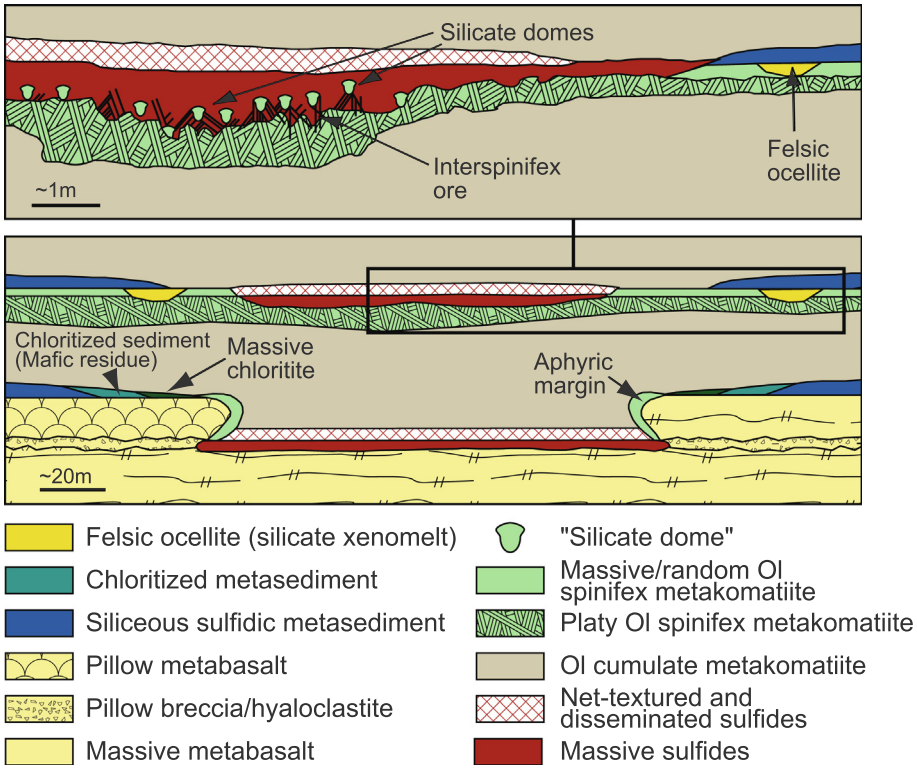

Fig. 2. Schematic section through a typical Kambalda ore environment after removal of superimposed deformation (modified from Gresham and Loftus-Hills, 1981; Lesher et al., 1981, 1984; Groves et al., 1986) showing contact ore localization in constructional embayment in footwall basalts (see Lesher and Barnes, 2009), local melting of lateral margins (pinchouts) and substrate by massive sulfides (Lesher et al., 1984; Lesher, 1989; Staude et al., 2016; Staude et al., 2017), local preservation of sediment xenomelts in flanking sheet-flow facies (Frost and Groves, 1989), and thermomechanical of the flow top and upper random spinifex zone of the lowermost host unit by sulfide melt at the base of an overlying flow unit, melting and displacing interstitial basaltic glass, forming silicate domes (Groves et al., 1986).

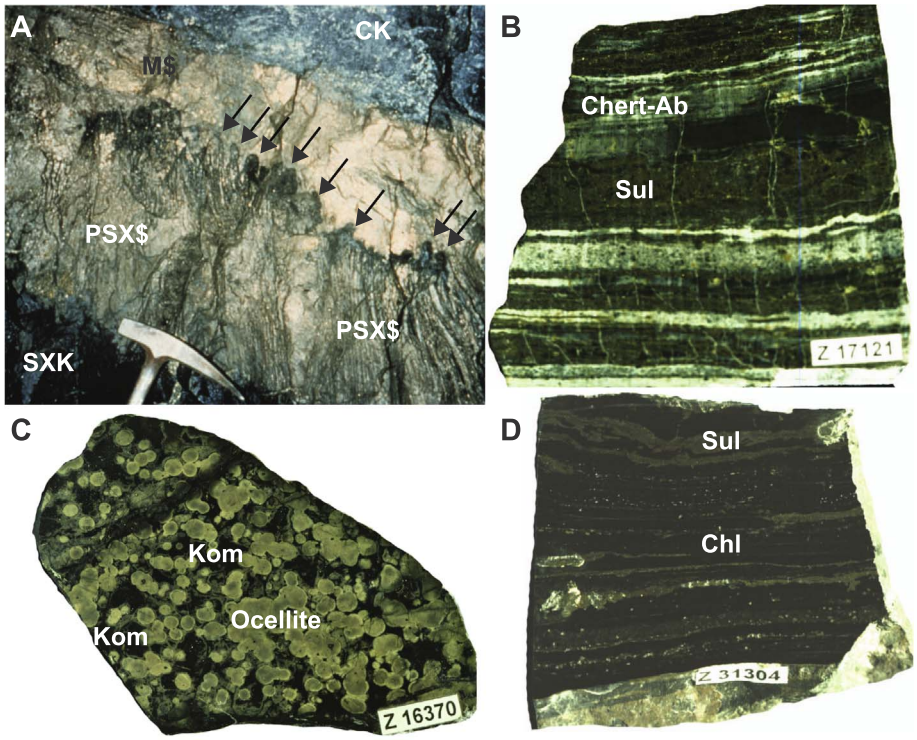

Fig. 3. A: Photograph of the erosional contact depicted in the upper part of Fig. 2, showing the erosional contact between an overlying mineralized komatiite flow (CK = cumulate komatiite) and a beheaded underlying komatiite flow, Lunnon 628 stope. Thermomechanical erosion has removed the upper flow-top breccia and random olivine spinifex zones of the flow (preserved along strike), massive Fe-Ni-Cu sulfide melt (M$) has melted, percolated downwards, and displaced basaltic interstitial melt between underlying platy olivine spinifex zone, forming spinifex-textured ore (PSX$) and basaltic silicate domes (arrows). Photo by MJ Donaldson. B: Photograph of a typical cherty sulfidic sediment at Kambalda. Light layers are chert-albite, brown layers are mainly pyrrhotite (Sul), and darker layers are chert-albite with fine-grained graphite. C: Photograph of a felsic "ocellite" (xenomelt) at Kambalda. Light globules are chert-albite, dark matrix is aphanitic to fine random olivine spinifex-textured komatiite (Kom). D: Photograph of a chlorite-sulfide rich sedimentary residue at Kambalda. Dark layers are mainly chlorite (Chl), brown layers are mainly pyrrhotite (Sul). E: Photograph of lower margin of the Katinniq Ultramafic Complex showing contact between basal pyroxenite (Pxnt), strongly recrystallized semipelite (HornA), and hornfelsed semipelite (HornB). Hammer is ~40 cm long. F: Photograph of fresh surface of strongly recrystallized semipelite. Pencil for scale. G: Photograph of fresh surface of hornfelsed semipelite. Pencil for scale. H: Photomicrograph of hornfelsed semipelite in G. Plane-polarized light. Width of photo is ~8 mm. I: Photograph of semipelite (slate) away from contact metamorphic aureole. Hammer is ~30 cm long. J: Photograph of semipelite (slate) in drill core showing dark colour (due to abundant fine graphite) and pyrrhotite-rich layers. K-L: Gabbroic melt films and diapirs along the contact between massive pyrrhotite-pentlandite-chalcopyrite and underlying gabbro, Katinniq. Height of images is ~60 cm. M: Irregular (erosional) photograph of a contact between massive pyrrhotite-chalcopyrite-pentlandite and argillite footwall rocks at Noril'sk. Blast hole is ~5 cm in diameter. N: Photograph of melted layers of argillite in massive in massive pyrrhotite-chalcopyrite-pentlandite. Blast hole is ~5 cm in diameter.

1) Many authors report ranges of −2 to +2‰ $\delta^{34}S$ for "mantle" S, but some authors report ranges as wide as −5 to +5‰ or more. Such ranges are normally derived from the S isotopic compositions of mid-ocean ridge basalts (MORB), which form by melting of asthenospheric mantle, but often misleadingly include the ranges for sulfate and sulfide, which fractionated on the seafloor after emplacement. When allowances are made for seafloor fractionation, the composition of MORB is extremely homogeneous at 0.1 ± 0.5‰ $\delta^{34}S$ (Sakai et al., 1984) or −0.91 ± 0.50‰ (Labidi et al., 2012), depending on the extraction method (Sn^{+2} + H_3PO_4 vs. HF + $CrCl_2$, respectively). The latter method has been argued to be more accurate, but most ore sulfides have been analyzed using the former method, so it is the more logical reference for the mantle range in Fig. 5. ^{33}S and ^{36}S isotopes in MORB are even more homogenous with mean values of −0.019 ± 0.005‰ $\Delta^{33}S$ (mass fractionation-corrected $\delta^{33}S$) and −0.193 ± 0.093‰ $\Delta^{36}S$ (mass fractionation-corrected $\delta^{36}S$), regardless of the extraction method (Labidi et al., 2012).
2) Some authors also include rare minor components of mantle (e.g., kimberlites) and analyses of individual phases (e.g., inclusions in diamond) in the ranges they report, but these components are not representative of the magmas that generate most magmatic Ni-Cu-PGE deposits. We know this because of the previous point: MORB is homogeneous because it forms at moderately high degrees of melting (10–15%) and is homogenized in the ridge-melting environment. The sulfide undersaturated picritic, komatiitic basaltic, ferropicritic, and komatiitic magmas that generated most high-grade Ni-Cu-PGE deposits formed at even higher degrees of partial melting (20–50%: e.g., Lesher and Stone, 1996; Arndt et al., 2005) and would have incorporated and homogenized even larger amounts of mantle. These magmas would have been just as close to 0‰ $\delta^{34}S$, $\Delta^{33}S$, and $\Delta^{36}S$ and just as homogeneous as MORB, and could not possibly have exhibited the more extreme values reported in some papers.
3) Just because an ore has a $\delta^{34}S$, $\Delta^{32}S$, or $\Delta^{36}S$ value similar to mantle, it does not mean that the S came from the mantle. It only means that the S isotopes in the source had not fractionated away from mantle values.
4) Mass-independent $\Delta^{33}S$ and $\Delta^{36}S$ values provide additional constraints where multiple Archean S sources are present and/or where mass-dependent fractions are limited (e.g., Bekker et al., 2009; Fiorentini et al., 2012a,b; Hiebert et al., 2013, 2016; Ding et al., 2012), but only mass-dependent $\delta^{34}S$ can be used in post-Archean rocks and mass-dependent fractionations provide important constraints on environmental conditions (oxidation state, biogenic activity).
5) S isotopes are sensitive to resetting in the dynamic magmatic systems that characterize deposits of this type, where $\delta^{34}S$ (as well as $\Delta^{33}S$ and $\Delta^{36}S$) values can be shifted toward mantle values with increasing magma:sulfide ratio (R factor) (e.g., Lesher and Stone, 1996; Lesher and Burnham, 2001; Ripley and Li, 2003), but they cannot be shifted away from mantle values by that process.

With these points in mind, the following features are evident in Fig. 5:

1) The S in most Ni-Cu-PGE deposits is significantly different from mantle S.
2) S isotopic compositions of ores are often intermediate between local wall rocks and mantle, consistent with formation from the wall rocks and subsequent exchange with the magma.
3) Where data are available for different zones within a deposit (e.g., Eagle: Ding et al., 2012; Sudbury: Ripley et al., 2015; Raglan: Lesher, 2007; Voisey's Bay: Ripley et al., 1999, 2002), S isotopic compositions often vary systematically from zone to zone, requiring variations in local sources and/or local variations in R factor.

Jinchuan and Nebo-Babel have been used as examples of deposits

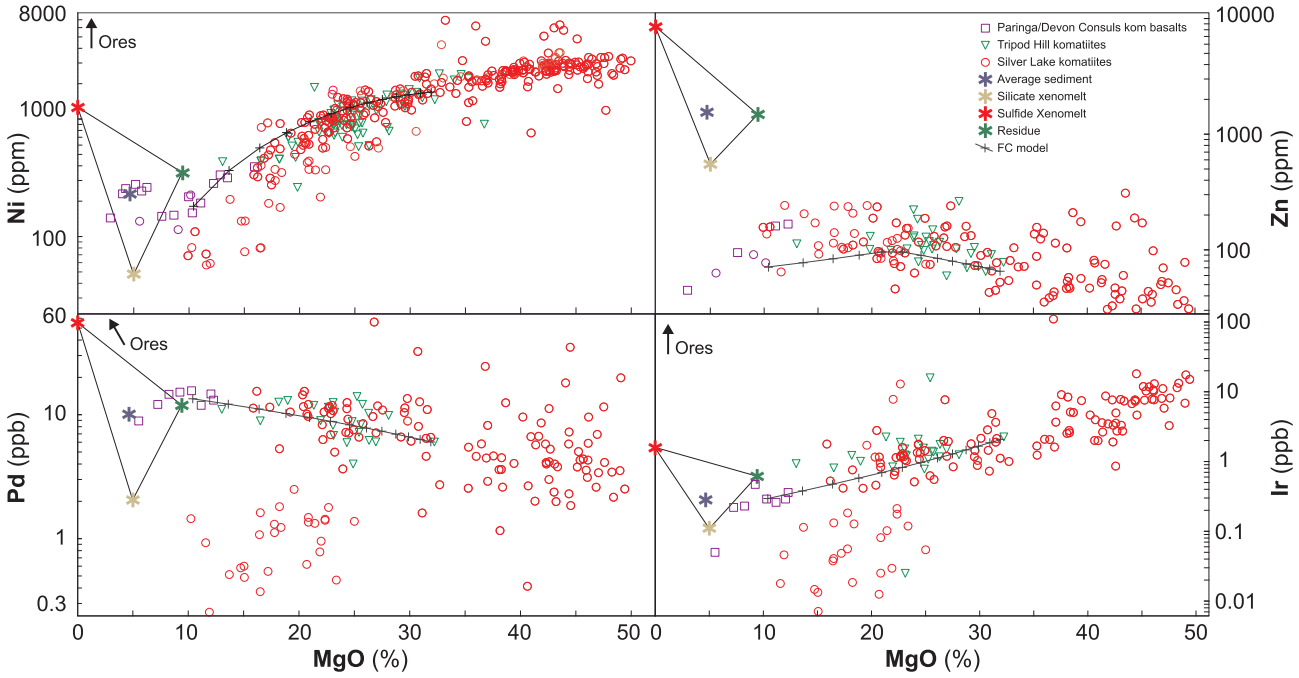

Fig. 4. Ni (A), Zn (B), Pd (C), and Ir (D) vs MgO plots showing compositional variations of Kambalda komatiites, komatiitic basalts, sediments, xenomelts, and residues (data sources in Lesher et al., 2001). The Silver Lake komatiite is composed of channelized sheet flows with thick lower olivine cumulate zones and thin upper spinifex-textured zones (not distinguished here to improve clarity, but all with > 30% MgO are ortho-mesocumulates and most with < 30% MgO are spinifex-textured). Most cumulate rocks are not contaminated (see discussion by Lesher and Arndt, 1995) or depleted in chalcophile elements (see Lesher et al., 2001), spinifex rocks in channel-flow facies are normally not contaminated or depleted in chalcophile elements, and spinifex rocks in sheet-flow facies are often contaminated and – as seen here – depleted in chalcophile elements. Overlying Tripod Hill komatiites (massive and spinifex-textured) and Paringa and Devon Consuls basalts are shown for reference. The computed fractional crystallization trend is after Lesher and Arndt (1995). The triangle defines an extract field formed by decoupling of silicate xenomelts (average felsic ocellite), residues (average chloritic sediments), and sulfide xenomelts (calculated) during melting of average sediment (see Lesher and Burnham, 2001 for calculation methodology). The chalcophile elements extracted from the depleted komatiites are interpreted to have upgraded the tenors of the sulfide xenomelts to produce the observed ore compositions (10–23% Ni, 1000–3500 ppm Pd, 150–500 ppm Ir, 200–400 ppm Zn: Cowden et al., 1986).

containing only mantle-derived S, based on near-mantle S isotopic compositions and the absence of abundant nearby crustal S sources (e.g., Chai and Naldrett, 1992; Seat et al., 2009), but Jinchuan is slightly but significantly more positive than mantle (see point 1 above) and S-rich metasediments have since been discovered in the region of Nebo-Babel (Karykowski et al., 2015). The S isotopic compositions of both were likely influenced by the R factor (see point 5 above).

Although a non-mantle origin for much of the S in many deposits was recognized early on, it was initially envisioned as a diffusive process involving incorporation of S released by conversion of pyrite to pyrrhotite (e.g., Naldrett, 1966; Ripley, 1981) and subsequently with more geological and fluid dynamic constraints as a wholesale assimilation process (e.g., Huppert et al. 1984; Lesher et al. 1984). However, it has since been appreciated that diffusion rates through wall rocks or xenoliths are much too slow (e.g., Robertson et al., 2015) and that the solubility of sulfide is much too low to dissolve the large amounts of sulfide in many deposits (0.1–0.3 wt% S in mafic-ultramafic magmas: e.g., Haughton et al., 1974; Shima and Naldrett, 1975; Mavrogenes and O'Neill, 1999), so the best model for most deposits is for an immiscible sulfide xenomelt to be released by melting wall rocks and upgraded by interaction with the magma (Lesher and Campbell, 1993). Sulfate can also be incorporated (e.g., Jugo et al., 2005), but must be reduced to sulfide (see discussion by Naldrett, 2004).

The composition of the sulfide xenomelt will vary depending on the nature of the source rock:

1) Sulfide facies iron formations (e.g., parts of the Duluth Complex, Forrestania, Shaw Dome) and evaporites (e.g., Noril'sk) normally contain little or no Ni-Cu-PGE or Cu-Zn-Pb
2) S-C-rich pelites/gneisses (e.g., other parts of the Duluth Complex, Raglan, Voisey's Bay) may contain trace to minor amounts of metals, more often Cu-Zn-Pb than Ni-Co-PGE
3) S-rich volcanic-exhalative rocks may contain significant amounts of Cu-Zn-Pb (e.g., Namew Lake: Menard et al., 1996)
4) Mafic-ultramafic rocks (e.g., Nipissing, East Bull Lake, and Archean Levack suite mafic intrusions at Sudbury) may contain significant amounts of Ni-Cu-(PGE)

Once incorporated, chalcophile elements will partition from (or rarely into) the silicate magma into (or rarely from) the sulfide xenomelt with the metal content of the final sulfide melt being controlled by 1) the abundance of metal in the initial sulfide xenomelt (Lesher and Burnham, 2001), 2) the abundance of metal in the initial silicate melt, 3) the sulfide melt/silicate melt partition coefficient (PGE $\ggg$ Cu > Ni > Co > Zn > Pb), and 4) the silicate melt/sulfide melt mass ratio (R factor) (Campbell and Naldrett, 1979). The abundances of metals and isotope ratios in all components of the system, the final sulfide melt, the final silicate melt, and any residues, xenoliths, xenocrysts, and xenovolatiles will be controlled by the same mass balances (see Lesher and Burnham, 2001). At high R the metal contents of all phases reach maxima/minima (depending on the relative abundances in the initial sulfide xenomelt and magma: see Figs. 6 and 7) and record true partition coefficients, whereas at lower R the metal contents of all phases are lower/higher and record only *apparent* partition coefficients (see Campbell and Barnes, 1984). Similarly, at high R the isotopic ratios of all phases approach the values in the initial magma, whereas at low R the isotopic ratios of all phases approach the values of the contaminants (Figs. 6 and 7). These models apply to batch equilibration or pooled dynamic equilibration. There are models that more closely simulate incremental dynamic upgrading (e.g., Brügmann et al., 1993), but the results are not significantly different except for elements with extremely high partition coefficients (see Naldrett, 2004).

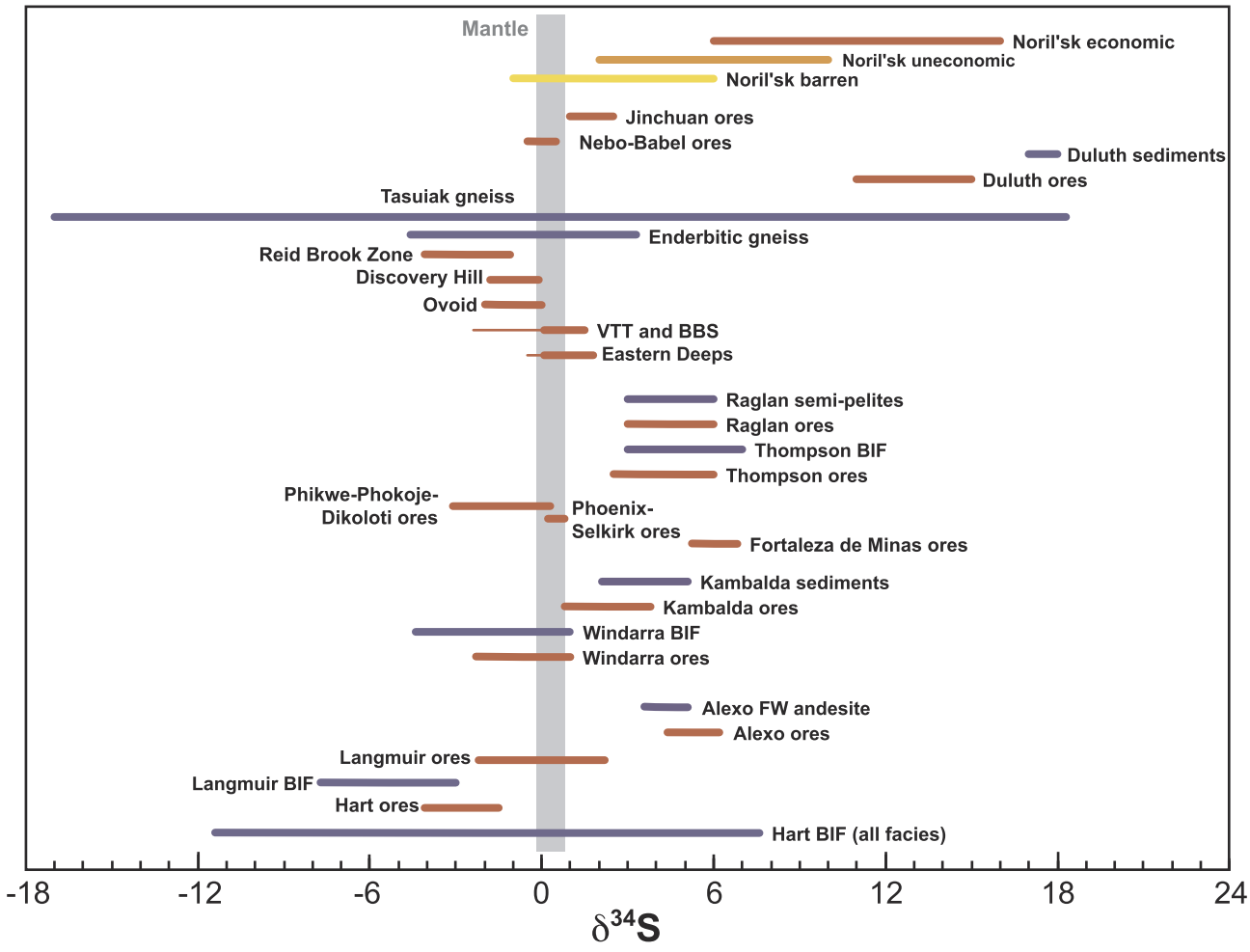

Fig. 5. $^{34}S/^{32}S$ isotopic data for selected Ni-Cu-PGE deposits. Data sources: Alexo: Naldrett (1966); Duluth: Mainwaring and Naldrett, 1977; Fortaleza de Minas: Choudhuri et al. (1997); Hart: Hiebert et al. (2016); Kambalda: Donnelly et al. (1978), Seccombe et al. (1981); Langmuir: Green and Naldrett (1981); Noril'sk: Grinenko (1985); Nebo-Babel: Seat et al. (2009); Phoenix-Selkirk and Phikwe-Phokoje-Dikoloti: Fiorentini et al. (2012a); Raglan: Lesher et al. (1999); Thompson: Bleeker (1990); Voisey's Bay: Ripley et al. (1999); Windarra: Seccombe et al. (1978).

4. Xenoliths

In many deposits (e.g., Duluth, Noril'sk, Sudbury, Voisey's Bay) xenoliths are closely associated with sulfide mineralization. They have traditionally been interpreted to represent wall rocks that contributed S (e.g., Mainwaring and Naldrett, 1977; Ripley, 1981; Thériault and Barnes, 1998; Samalens et al., 2017) and sometimes metals (e.g., Tyson and Chang, 1984), but played mainly a passive role during sulfide transport and deposition, reflecting hydrodynamic equivalence (e.g., Li and Naldrett, 2000) where less dense but larger silicate xenoliths have similar settling rates as denser but smaller sulfide droplets.

However, as we shall see they may have played more active roles by: 1) increasing bulk viscosity, 2) reducing bulk density if less dense than the magma or increasing bulk density if more dense than the magma, and if olivine-rich and if silicate melt can be advected away, 3) providing a medium for sulfide melt droplets to nucleate, allowing sulfide to be more easily transported upwards. Even if they contain no S, inclusions may contaminate the invading magma, potentially lowering sulfide solubility, but because of the limits on the solubility of sulfide in magmas noted above and the even greater limits on the changes in solubility with contamination, this normally generates only small amounts of sulfides.

Xenoliths are very rare and occur only along the basal contacts at Kambalda (e.g., Frost and Groves, 1989a), which formed from a very high-T (~1620 °C) komatiitic magma, although they have been reported in komatiitic rocks at Digger Rocks (Perring et al., 1995) and Hunters Road (Prendergast, 2001). They are rare and only occur along the basal contact with gabbros (but not metasediments) at Raglan (e.g., Lesher, 2007), which formed from a intermediate-T (~1360 °C) komatiitic basaltic magma. However, xenoliths are common at Duluth, Noril'sk, and Voisey's Bay, which formed from lower-T (< 1280 °C) picritic/basaltic magmas and at Sudbury, which formed from a low-T (~1180 °C at the liquidus) quartz dioritic magma. Several examples are described below.

4.1. Sudbury

Xenoliths are common in both Contact Sublayer (Fig. 8A) and Offset Sublayer (Inclusion-Rich Quartz Diorite) (Fig. 8B) at Sudbury. They range from felsic to ultramafic in composition, but mineralization is more commonly associated with mafic-ultramafic inclusions (e.g., Pattison, 1979; Naldrett et al., 1984; Lightfoot et al., 1997; Prevec et al., 2000). The melt sheet at Sudbury has been interpreted by most workers to have been initially superheated (up to 2000 °C: Ivanov and Deutsch, 1999), so the preserved inclusions must have incorporated at a later stage – after earlier inclusions had been digested and cooled the melt sheet closer to the liquidus (~1180 °C). It is not yet clear how many represent cognate inclusions (Lightfoot et al., 1997; Prevec et al., 2000), xenoliths of local contact rocks (e.g., Pattison, 1979), or exotic xenoliths (e.g., Naldrett et al., 1984), but some exhibit evidence of shock

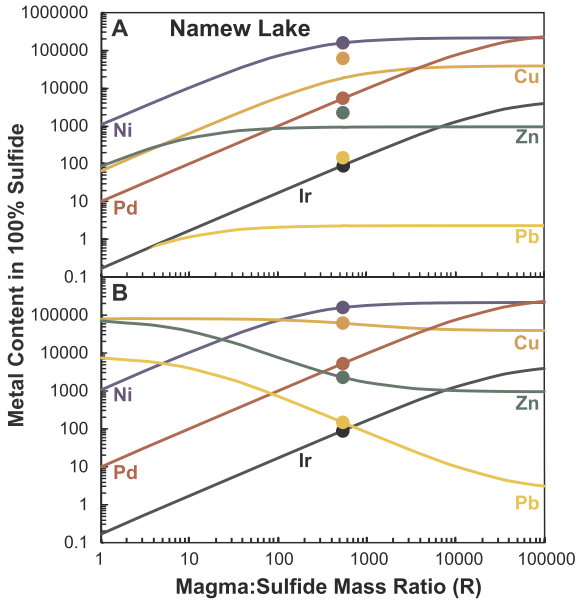

Fig. 6. R factor mixing models for Ni-Cu-PGE mineralization at Namew Lake, Manitoba using the model of Lesher and Burnham (2001). Curves are calculated variations with R, assuming 1080 ppm Ni, 65 ppm Cu, 10 ppb Pd, 0.17 ppb Ir, 95 ppm Zn, and 0.23 ppm Pb in the initial komatiitic magma, $D_{Ni}^{Sul/Sil}$ = 200; $D_{Cu}^{Sul/Sil}$ = 600, $D_{Pd}^{Sul/Sil}$ = $D_{Ir}^{Sul/Sil}$ = 30,000, $D_{Zn}^{Sul/Sil}$ = 10, and $D_{Pb}^{Sul/Sil}$ = 10. Dots are average NL ore compositions (Menard et al., 1996). Ni-Cu-Zn-Pb in ppm, Pd-Ir in ppm. A: Variations assuming no metals in the initial sulfide xenomelt. This model accounts for the abundances of Ni-Pd-Ir in the deposit, but does not account for the anomalously high Cu-Zn-Pb abundances in the deposit. B: Variations using same magma but assuming initial sulfide xenomelt (volcanic-exhalative rocks) contained no Ni, Pd, or Ir, 8.1 wt% Cu, 7.5 wt% Zn, and 0.8 wt% ppm Pb. This model fits the data (RMSD = 1.68) at an R value of 538.

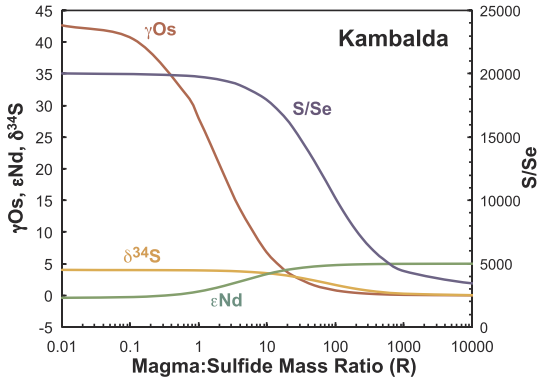

Fig. 7. R factor isotopic mixing models for Kambalda, Western Australia (summarized from plots in Lesher and Burnham, 2001). At low R the isotopic values converge to those in the initial sulfide xenomelt; at high R the isotopic values converge to those in the mantle-derived magma. Because of differences in the isotopic ratios and abundances in the different systems, they mix along different trajectories with γOs isotopes converging to near-mantle values at the lowest R factors, εNd (silicate components) at intermediate R factors, and δ ^{34}S and S/Se converging at the highest R factors. The R factors at Kambalda have been estimated independently to be within the range 100–500 (Lesher and Campbell, 1993).

metamorphism (Wang et al., 2016a) and are clearly not cognate, and some contain abundant phlogopite and are clearly exotic (Wang et al., 2016b).

The strong association between ultramafic inclusions, mineralization, and embayments in the contact environments at Sudbury can be explained in two fundamentally different ways: 1) a mixture of SIC melt, Fe-Ni-Cu sulfide melt precipitated from the overlying melt sheet, and ultramafic inclusions derived from footwall rocks accumulated along the basal contact and was swept into pre-existing embayments by convection currents (e.g., Keays and Lightfoot, 2004) or slumped into the embayments as dense debris flows, and/or 2) all three are the products of local thermomechanical erosion of pre-existing protores in Nipissing, East Bull Lake, and Levack Gneiss suite intrusions. The latter interpretation is supported by the close association between mineralized embayments and mafic-ultramafic footwall rocks (Lightfoot, 2016), the compositional similarities[2] between Nipissing-hosted Ni-Cu-PGE ores (see data in Sproule et al., 2008) and average Sudbury ores (see data in Lightfoot, 2016), systematic variations in Pb isotopic compositions (see data and discussion by McNamara et al., 2017), and systematic variations in S isotopic compositions (see data in Ripley et al., 2015).

The strong association between inclusions and mineralization in the subvertical offset dike environments at Sudbury (see review by Lightfoot, 2016) suggests that the inclusions increased the effective viscosity of the quartz dioritic (QD) magma, inhibiting coarse (2–3 cm) disseminated and semi-massive Fe-Ni-Cu sulfide melts from settling.

[2] Although the quartz dioritic melt contained less Ni and Cu than the Nipissing magma, this would be offset by the higher sulfide/silicate partition coefficients expected in a more polymerized quartz dioritic melts (see discussion by Lesher and Arndt, 1995; Lesher and Campbell, 1993). This means that even if magma:sulfide ratios (R factors) varied widely, the compositions would not change significantly, explaining the relatively narrow ranges of metal tenors in Sudbury contact ores (see Lightfoot, 2016).

The absence of inclusions or mineralization in the thin (20 cm – 1 m wide) lateral margins of the dikes (Fig. 8C) and the presence of inclusions of barren QD within IQD (Fig. 8C) suggests two phases of emplacement (Lightfoot et al., 1997). The occurrence of IQD in the interior and only rarely along the margins of the dikes suggest that the interiors must have been mechanically weak and therefore not completely crystallized, implying rapid sequential emplacement of QD and IQD and therefore very rapid achievement of sulfide saturation (Lesher, 2013c), not slow exsolution and gravitational settling during cooling of the Main Mass (e.g., Keays and Lightfoot, 2004; Li and Ripley, 2005).

4.2. Voisey's Bay

The xenoliths at Voisey's Bay appear be derived from the pelitic paragneiss, enderbitic orthogneiss, and mafic to quartzofeldspathic gneiss country rocks, which have been contact metamorphosed and partially melted by the magma: garnet oxidized to hercynite and magnetite, adding Si to the magma; cordierite dehydrated to hercynite, adding Si to the magma; hypersthene and K-feldspar reacted to produce hercynite, adding of Si and K to the magma; plagioclase broke down to corundum, adding Si and Na to the magma; and corundum reacted with Fe and Mg in the magma to form additional hercynite (Li and Naldrett, 2000; Mariga et al., 2006). This increased the density of the inclusions, explaining the close association between the inclusions and sulfide ores (Naldrett, 1966). Some are plagioclase-rich (S.J. Barnes, pers. comm., 2017), but are not concentrated in the upper parts of the chambers so were likely still denser than the magma or trapped by the sulfide melt before they could segregate (see Discussion below). This made the sulfide-xenolith mixture even denser than the mafic magma and less likely that the inclusions and sulfides moved upwards through the system (cf. Lightfoot et al., 2012) and more likely that they settled backwards in the system (see Discussion below and Barnes et al., 2017).

4.3. Black Label hybrid zone

The Blackbird – Black Thor Igneous Complex (BTIC; also known as the "Double Eagle Complex) in the McFaulds Lake Greenstone Belt of northern Ontario contains significant Ni-Cu-PGE mineralization within footwall feeder dikes/sills at Eagle's Nest (Mungall et al., 2010) and Bluejay (formerly AT-12), and minor low-grade mineralization within cognate breccias along the periphery of a late websterite phase emplaced into the Black Label chromite zone (Farhangi et al., 2013; Spath et al., 2015; Spath, 2017). The spatial association and textures indicate

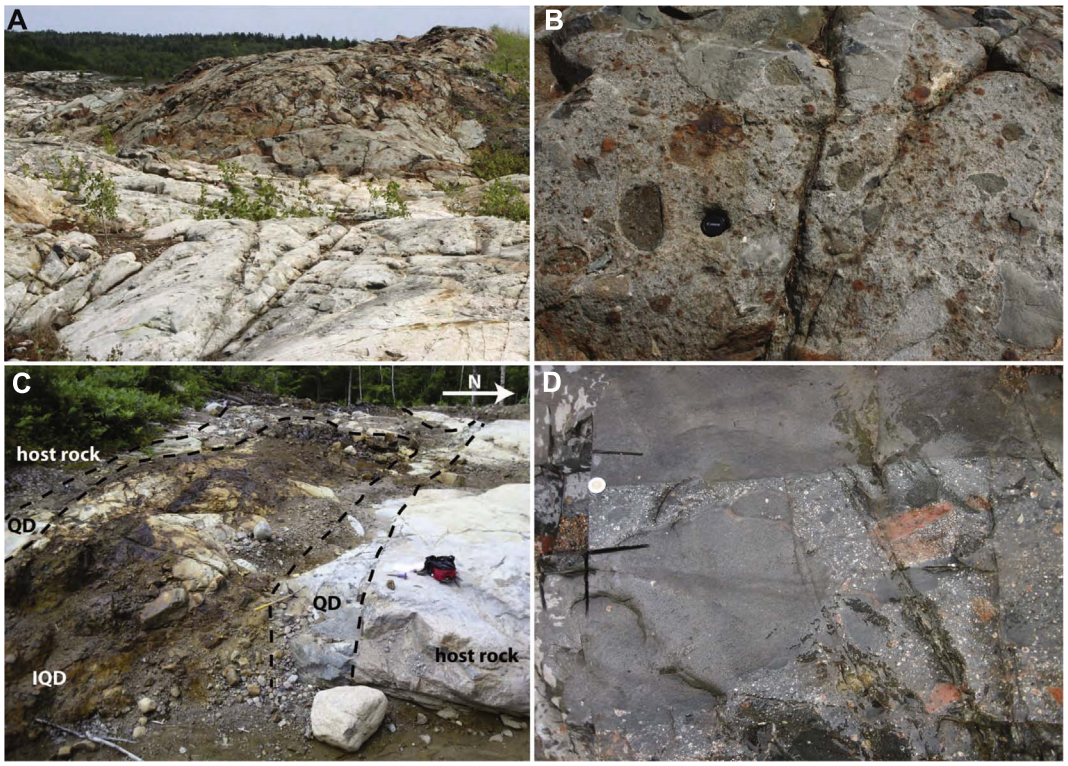

Fig. 8. A: Photograph of Contact Sublayer/Granite Breccia contact, Whistle Embayment, Sudbury Photograph of inclusion-rich Contact Sublayer, Whistle Embayment, Sudbury. B: Close-up of Contact Sublayer in central part of A showing rounded mafic-ultramafic clasts and disseminated Fe-Ni-Cu sulfides. Lens cap is 76 mm in diameter. C: Photograph of western part of Trill Offset Dike. Sudbury (photo by L-M Klimesh) showing mineralized inclusion quartz diorite (IQD) core and unmineralized inclusion-free quartz diorite (QD) margin. Backpack is ~60 cm long. D: Contact further east in Trill Offset Dike showing sharp transgressive contact between barren QD (upper part) and weakly mineralized IQD (lower part) containing inclusions of QD and felsic country rocks. Coin is 28 mm in diameter.

that the mineralization formed by reaction of the late websterite magma with previously crystallized parts of the BTIC. Although there are many examples where minor amounts of Ni-Cu-PGE mineralization are associated with breccias and/or partial melts along the margins of mafic-ultramafic intrusions (e.g., East Bull Lake: Peck et al., 2001; Platreef: Kinnaird et al., 2005; River Valley: Holwell et al., 2014), this is the first case known to me where Ni-Cu-PGE sulfide mineralization – albeit small amounts with low grades – has formed through interaction of a magma with *cognate* xenoliths.

5. Silicate xenomelts

Silicate xenomelts are rarely preserved, because they are normally miscible in the lava/magma and are easily assimilated in dynamic systems, but they have been preserved in a few localities, including:

1) Xenomelts of sediments preserved as ocellar rocks in the upper parts of flanking sheet-flow facies at Foster Shoot, Kambalda (e.g., Frost and Groves, 1989b). They are depleted in S and metals, which appear to have been sequestered by the complementary sulfide xenomelts (Fig. 4).
2) Xenomelts of argillites within massive ores at Noril'sk (Fig. 3K)
3) Xenomelts of felsic volcanic rocks preserved as diapirs and films along the lower contacts of the host units at Silver Swan (Dowling et al., 2004).
4) Xenomelts of gabbros preserved along the margins of xenoliths and as films along the lower contact at Katinniq (Fig. 3L-M).
5) Xenomelts of basalts preserved as accumulations along the basal sulfide-basalt contact and along the upper margins of ore pinchouts at Kambalda (see Frost and Groves, 1989; Staude et al., 2016, 2017).

The Duluth Complex contains numerous iron oxide-rich dikes, sills, pods, and, pipelike bodies (e.g., Mainwaring and Naldrett, 1977; Ripley et al., 1998). Ripley et al. (1998) suggested that the oxide-apatite-rich rocks were the products of liquid immiscibility, but it is possible that the iron oxide-rich bodies represent the residues (liquids and/or solids) of partial melting of Biwabik Iron Formation with Ti partitioning into the oxide-rich residue and contamination triggering apatite saturation. The present distribution of sulfide and oxide deposits in the lower part of the Duluth Complex does not correspond to their proximities to S-rich Virginia Formation or Fe-rich Biwabik Iron Formation (see Ripley et al., 1998), but the two mineralization types are strongly segregated along strike (Cu-Ni-PGE to the north, Fe-Ti oxide to the south), so it seems possible that they represent accumulations from those sources but that the current erosional section does not reflect the locations of those sources during incorporation (i.e., that the contact geometry is misleading and/or that further erosion has modified the location of the contact).

6. Xenocrysts

Xenocrysts appear to be less often preserved (or recognized), but chromite and olivine xenocrysts are present in the Black Thor Igneous Complex (Spath et al., 2015; Spath, 2017), garnet xenocrysts are preserved at Savannah (S.J. Barnes, pers. comm., 2017), and quartz and plagioclase xenocrysts are preserved at Nebo-Babel (Seat et al., 2007).

As noted above, the abundant chromite in the Black Thor Igneous Complex has been interpreted to represent xenocrystic magnetite that has been converted to chromite by interaction with the Cr-rich parental komatiitic magma (Fig. 9). If this interpretation is correct, the model may apply to varying degrees to other chromite deposits that are hosted in magmatic conduits (e.g., Inyala, Ipueira-Medrado, Kemi, Nkomati, or Sukinda) and explain why the chromite horizons in those deposits are so thick.

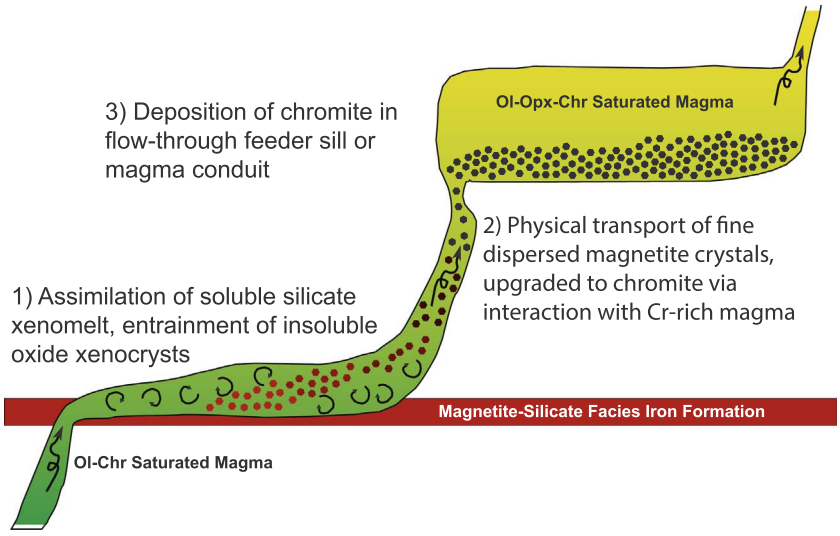

Fig. 9. Schematic model for dynamic upgrading of iron-formation magnetite (or ilmenomagnetite from gabbro) to chromite (Lesher et al., 2014, submitted).

7. Xenovolatiles

The S sources at some Ni-Cu-(PGE) deposits (e.g., Jinchuan, Sudbury, Thompson, Voisey's Bay) were consolidated and more-or-less anhydrous at the time of incorporation and the ores in those localities do not appear to contain any vesicles or amygdales (Fig. 10A-B).

However, the S sources at other Ni-Cu-(PGE) deposits (e.g., Alexo-Dundonald, Kambalda, Noril'sk, Pechenga, Raglan) were unconsolidated at the time of incorporation and these ores are locally vesicular/amygdaloidal (Fig. 10C; see review by Barnes et al., 2017). Ore formation involving unconsolidated sediments and volcaniclastic rocks would have been very dynamic, as they were fluidized and/or volatilized, aiding mechanical erosion and facilitating assimilation (e.g., Williams et al., 1998, 2002; Le Vaillant et al., 2017), and ultimately partially melted and devolatilized, producing sulfide xenomelts and supercritical xenofluid/gas bubbles.

8. Residues and skarns

Although the wall rocks bordering magmatic ore deposits are commonly contact metamorphosed and sometimes partially melted (e.g., Alexo: Houlé et al., 2012; Kambalda: Frost and Groves, 1989a; Staude et al., 2016, 2017; Noril'sk: e.g., Naldrett, 2004; Raglan: Lesher, 2007; Sudbury: e.g., McCormick et al., 2002), residues of devolatilization/partial melting/reaction appear to be less well preserved.

Because the rate thermomechanical erosion of wall rocks and inclusions is much faster than the rate of heat conduction (see discussion by Huppert et al., 1984; Williams et al., 1998), the rocks or parts of an inclusion adjacent to an actively eroding contact will remain at more-or-less ambient conditions until eroded. Only after erosion ceases – due to temperature or magma dynamics – will the thermal aureole expand in thickness. With all else equal a contact metamorphic aureole adjacent to a body emplaced into more rapidly-cooled volcanic environment will be narrower than an aureole adjacent to a body emplaced into a more slowly-cooled subvolcanic or plutonic environment, and the aureole adjacent to thicker body will be wider than the aureole adjacent to a thinner body, but the nature of the wall rocks is equally important. This explains the differences between the very thick aureoles at Sudbury (2-pyroxene hornfels in basalts up to 750m from the contact from the 2–3 km-thick melt sheet), the thick aureoles at Noril'sk (metasomatic zones up to 300 m wide in argillites and evaporates adjacent to < 300 m-thick intrusions), the thin aureoles at Raglan (biotite in semi-pelites up to 10 m below 200 m-thick lava channels), and the very thin aureoles at Kambalda (negligible contact metamorphism in basalts beneath 30-100m thick lava channels).

Three examples are described here: 1) residues at Kambalda, 2) contact metamorphosed footwall rocks at Raglan, and 3) skarns at Sudbury.

9. Kambalda residues

The residues of devolatilization of cherty sulfidic sediments at Kambalda occur as chlorite- and sulfide-rich metasediments on the mid-proximal parts of the contacts flanking the ore-localizing embayments that are depleted in $Na \gg Ti \sim Sr \sim Al \sim Y > Zr \sim Si \sim U > Th > P$ and enriched in $Cr < Mg < Zn < Ca < Ir \sim Pd \sim Fe \sim Ni < Mn < Co < S \sim Cu < Au$ relative to precursor sediments. Bavinton (1981) interpreted them to be primary sedimentary rocks that contained less felsic components and more basaltic components, but Lesher and Burnham (2001) interpreted them as devolatilized cherty sulfidic metasediments based on their similar refractory lithophile element ratios and their intermediate position flanking the main lava channels – between a more proximal zone where only a thin (~10–20 cm) zone of massive chlorite is preserved and a more distal zone where contact sediments are preserved (Fig. 2). Their geochemical characteristics, including metal contents (Fig. 4), and mass balance constraints (see discussion in Lesher and Burnham, 2001), suggest that they represent more refractory mafic components after removal of less refractory felsic components, presumably represented by rare felsic ocellites (Frost and Groves, 1989b). Staude et al. (2017) describe cm-scale layer-specific melting of the contact sediment at Moran Shoot by infiltrating sulfide where the cherty layers did not melt and the aluminous layers melted completely to form melt emulsions with the sulfide, but only within mm of the contact. The degree of melting clearly varied with the thermal history of the lava channel and the composition of the sediment.

The presence of pyrrhotite in devolatilized chlorite-rich sediments directly beneath the lavas at Kambalda (Fig. 3D) and in metamorphosed xenoliths in other deposits (e.g., Duluth, Voisey's Bay), indicates that it was more stable than some of the felsic components during contact metamorphism. Pure $Fe_{1-X}S$ melts at ~1190 °C, higher than the melting point of wet felsic components. $(Fe, Ni, Cu)_{1-X}S$ melts at temperatures as low as ~900 °C (e.g., Kullerud et al., 1969). Solid-state diffusion rates are generally much slower than melting rates (see discussion by Robertson et al., 2015), so even if pyrrhotite was incorporated into the magma where Ni-Cu would be able to diffuse into the margins of the clasts, this would occur at rates much slower than melting. As noted above in some deposits the sulfide that was incorporated contained significant amounts of Cu-Zn-Pb (e.g., Namew Lake) or Ni-Cu (e.g., Sudbury) and would have melted at lower temperatures.

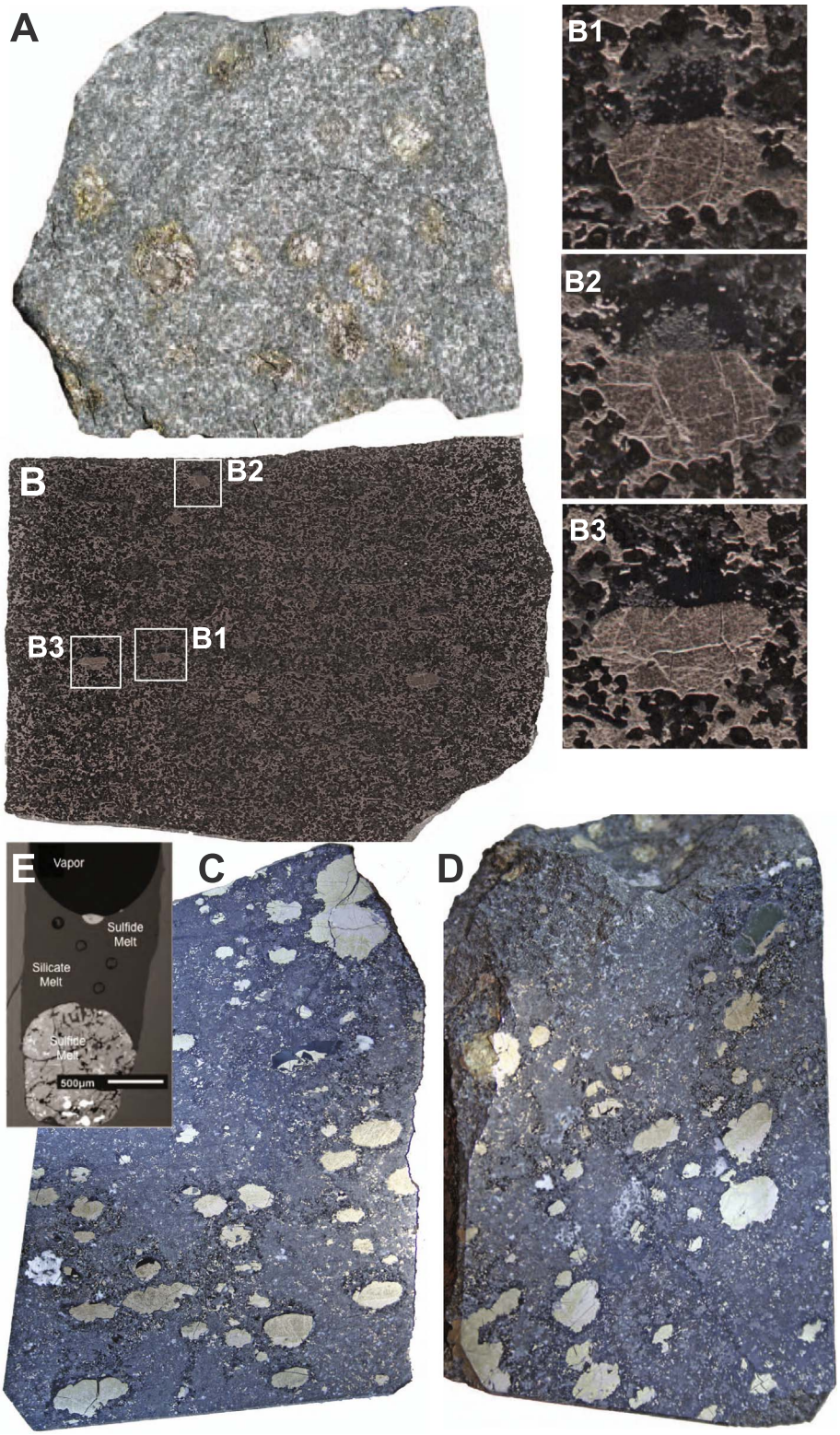

Fig. 10. A: Coarse (2–3 cm) disseminated Po-Pn-Ccp droplets in quartz diorite, Copper Cliff North Mine, Sudbury. Note absence of any associated silicate melt or former volatile components. B: Intermediate-sized (1–2 cm) composite sulfide-silicate droplets in net-textured ore, Katinniq deposit, Raglan. Silicate caps are igneous pyroxene and chlorite after komatiitic melt, not secondary phases filling vesicles. Lower margins conform to underlying olivine (now serpentine-magnetite), indicating some settling. C and D: Coarse (up to 3 cm), slightly flattened composite sulfide-silicate globules in varitextured "taxitic" gabbro, Bear's Brook open pit, Noril'sk I mine. Note light-green to grey chalcedonic upper parts of many globules, which is a secondary vesicle filling. E: Analogous composite sulfide-vapor bubble at the top of an experimental capsule (Mungall et al., 2015).

9.1. Raglan footwall rocks

The footwall rocks at Raglan include metapelites and metagabbros (see review by Lesher, 2007). The metapelites provide the best information regarding thermal gradients: they are strongly recrystallized and metasomatized to fine-grained massive light green granofels within 1m of the contact (Fig. 3E-F), metamorphosed to white and brown spotted biotite hornfels 1–5 m from the contact (i.e., higher T than the ambient chlorite zone lower greenschist facies metamorphism) (Fig. 3G-H), and are virtually unhornfelsed black graphitic-sulfidic slates > 10 m from the contact (Fig. 3I-J). The proximal granofels facies is so massive and so strongly recrystallized that it was mapped by some early workers as basalt. The bleaching is similar to that observed at Alexo (Houlé et al., 2012) and Sothman (Houlé and Lesher, 2011), and has been interpreted to reflect ponding of hot fluids released from unconsolidated to semi-consolidated sediments (Raglan) and porous

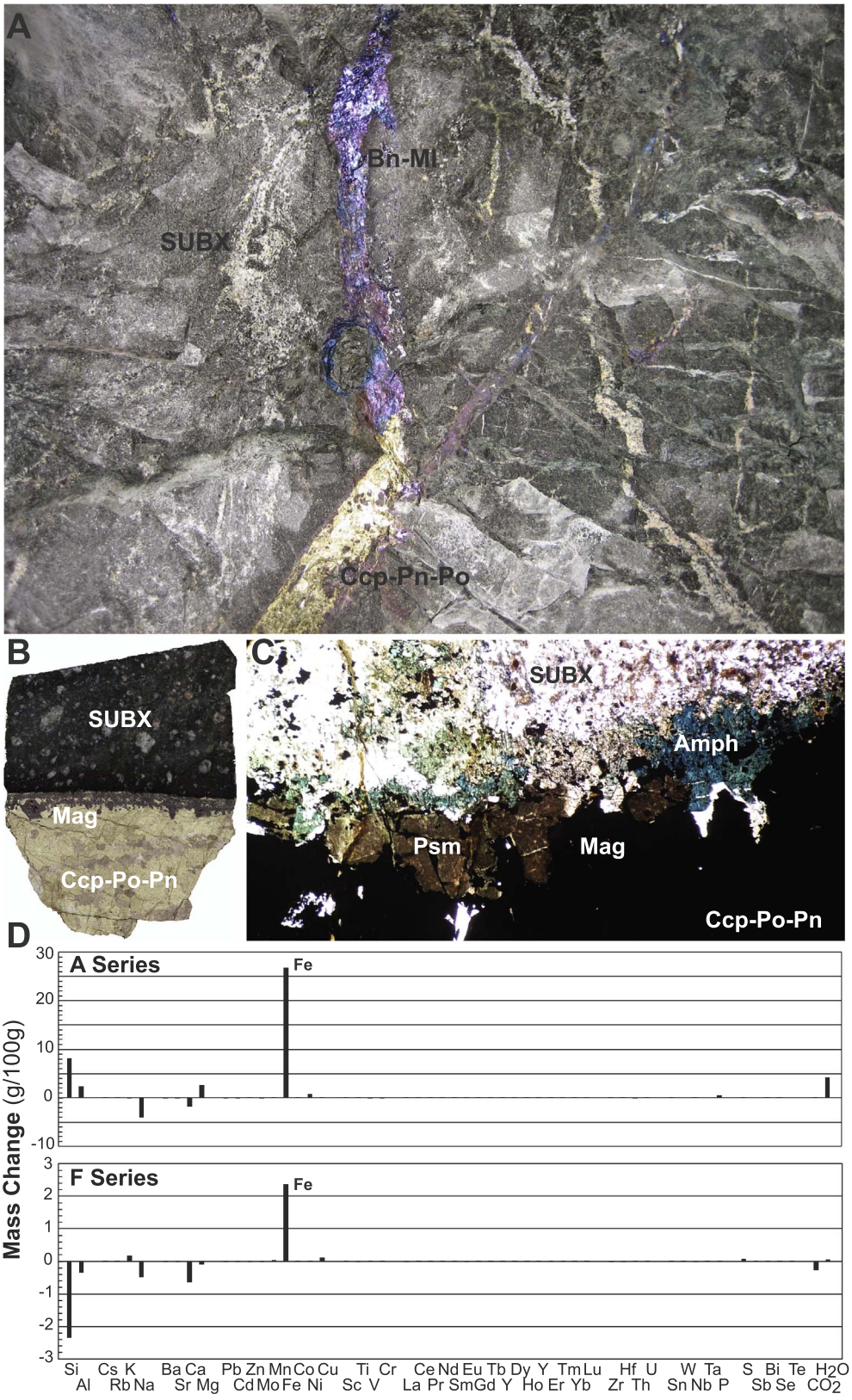

Fig. 11. A: Photograph of mine face containing a massive sulfide vein in Sudbury breccia (pseudotachylitic Levack Gneiss) grading from chalcopyrite-pentlandite into a bornite-millerite, McCreedy East 153 deposit, Sudbury. B: Photograph of the margin of a footwall Fe-Cu-Ni sulfide vein, McCreedy East 153 ore body, Sudbury. Note very thin alteration selvedge and thick margin of skeletal magmatic magnetite. C: Photomicrograph of similar margin in same area showing actinolite and pyrosmalite (analysis: $Fe_{7.9}\ Mg_{0.09}\ Mn_{0.03}\ Si_{6.3}\ O_{15}\ (OH)_{13}$) – interpreted to be a pseudomorphous after pyroxene – along the margin. D: Density-weighted enrichment-depletion diagram showing mass changes between two alteration selvedges in the same area. B-D from Raskevicius (2013).

volcanic rocks (Alexo, Sothman) beneath the host units. In all of these cases, the degree of metamorphism is greater around the embayments, suggesting that this is related to lava channelization, not simply post-magmatic contact metamorphism, which would have progressed much more slowly (see discussion by Robertson et al., 2015). The key could have been fluids ponded beneath the submarine lava channels, which could have permitted heat to be conducted much more rapidly than through dry rocks – allowing the footwall rocks to "stew" in their own juices.

9.2. Sudbury skarns

Thin (1–3 cm) actinolite-magnetite-sulfide selvedges bordering footwall Fe-Cu-Ni sulfide veins at Sudbury (Fig. 11A-B) have historically been interpreted to be hydrothermal/metamorphic reaction zones (e.g., Farrow and Watkinson, 1997), but Nelles (2012) and Raskevicius (2013) interpreted them as reaction skarns between Fe-Cu-Ni sulfide melt and felsic wall rocks (in most cases impact-generated pseudotachylitic breccias derived from Levack Gneiss). Density-weighed mass balance calculations (Fig. 11C) indicate the major change is the transfer of Fe from the sulfide melt into the wall rock.

The significance of this to ore genesis is that the vein systems are zoned from chalcopyrite – pyrrhotite – pentlandite proximal parts to bornite ± millerite-rich peripheral parts. This is commonly interpreted to represent hydrothermal mobilization from the contact ores (e.g., Farrow and Watkinson, 1997), but there are many problems with such an interpretation:

1) The selvedges are too narrow to represent fluid-rock interaction by the very large amount of fluid that would be required to transport and deposit such large amounts of Fe-Cu-Ni sulfides.
2) Fe is normally much more soluble in hydrothermal fluids than Cu and considerably more soluble than Ni in the absence of As (which is only a trace component on the North Range). Although there are some Fe-Cu sulfides in the selvedges and surrounding wall rocks, the abundances are very much lower than in deposits known to have been deposited from hydrothermal fluids (e.g., VMS and porphyry Cu deposits).
3) Much of the vein mineralization contains small but significant amounts of Ir, whereas Ir is below detection limits in unequivocal hydrothermal Fe-Cu-Ni sulfides (e.g., Lesher and Keays, 1984).
4) Experimentally-determined phase equilibria in the Fe-Cu-S (Fig. 12A) and Fe-Ni-S systems (see review by Naldrett, 2004) indicate that there is a thermal minimum near the composition of ISS and do not permit formation of significant amounts of bornite ± millerite-rich along normal liquid lines of descent.

The best interpretation is that reaction of Fe-Cu-Ni sulfide melt with the felsic wall rocks and loss of Fe drove the liquid into primary phase volumes of bornite solid solution and/or millerite (Fig. 12B).

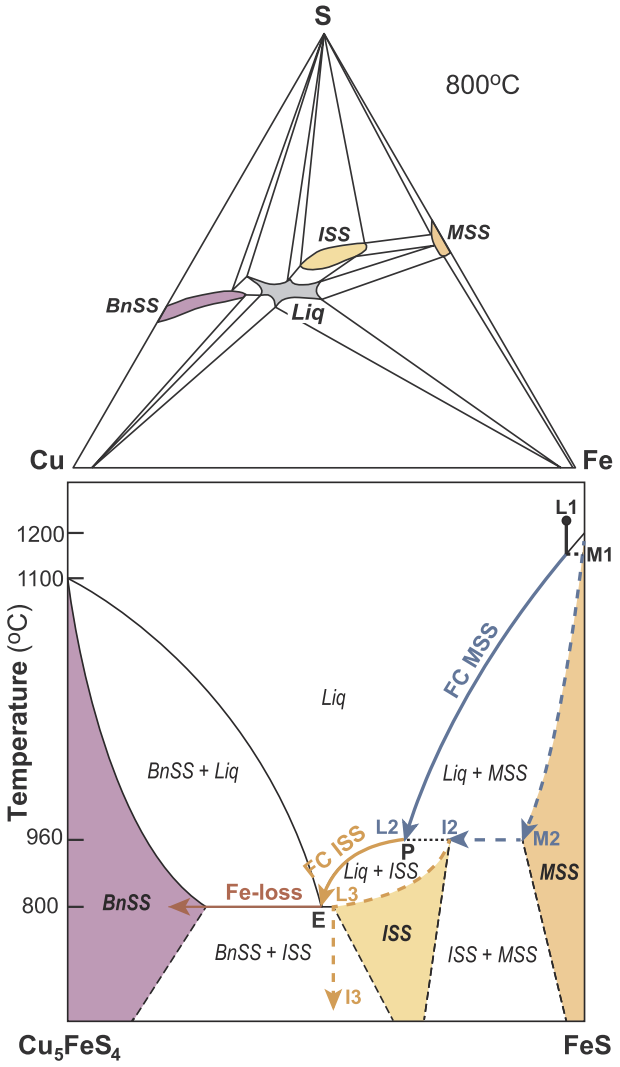

Fig. 12. A: Phase diagram at 800 °C in the Fe-Cu-S system (redrawn from Tsujimura and Kitakaze, 2004). **BnSS**: bornite solid solution, **MSS**: monosulfide solid solution (pyrrhotite solid solution), **ISS**: intermediate solid solution, **Liq**: Fe-Cu-S liquid, **P**: peritectic, **E**: eutectic. Note that the liquid field represents the thermal minimum in this system and that it lies between MSS – ISS and BnSS. A sulfide liquid with a composition similar to unfractionated Sudbury contact ores would contain ~5% Cu and would fractionate MSS and then ISS, not reaching the field where BnSS would crystallize. Removing Fe (in magnetite and Fe-rich silicates) would drive it toward the field where BnSS would crystallize. **B**: Schematic section between Cu_5FeS_4 (bornite solid solution) and FeS (MSS) (from Nelles and Lesher, in revision), showing the trajectory of the sulfide melt during crystallization of MSS and ISS, and the effect of removing Fe in magnetite and Fe-silicates. **L1**: initial sulfide melt, **M1**: MSS in equilibrium with L1, **L2**: sulfide melt at MSS-ISS peritectic P, **M2**: MSS in equilibrium with L2, **I2**: ISS in equilibrium with L2, **L3**: sulfide melt at eutectic E, **I3**: ISS in equilibrium with L3.

10. Discussion

The three most important constraints on the role of xenophases in the genesis of Ni-Cu-PGE mineralization are 1) the viscosity of the silicate magma, 2) their survival times, and 3) their influence on the transport of dense sulfide melts and/or oxides.

10.1. Viscosity

The ascent rates of basaltic and ultramafic magma are controlled mainly by density contrasts with the wall rocks and magma viscosity. Whereas the densities of anhydrous basaltic and ultramafic magmas vary narrowly within the range 2.7–2.8 g m^{-3}, viscosities range more widely within the range 1–1000 g cm^{-1} s^{-1} and even higher if the abundances of xenophases are high enough to increase their effective viscosities. There are many formulations (see review by Petford, 2009), but assuming spherical particles and hexagonal-closest packing (Shaw, 1972) viscosity increases one order of magnitude with ~45% xenoliths/xenocrysts, two orders of magnitude with ~62% xenoliths/xenocrysts, three orders of magnitude with ~69% xenocrysts, four orders of magnitude with ~72% xenoliths/xenocrysts, and reaching infinite viscosity at ~74% xenoliths/xenocrysts. As a consequence, xenocryst/xenocryst-rich magmas may ascend slowly even if the xenocrysts/xenoliths are less dense than the magma.

However, viscosity also influences the sinking/floating velocities of xenophases. The very high effective viscosities of congested suspensions is one of the explanations for why there is so little segregation of less dense xenoliths/xenocrysts from much denser sulfide melts in most magmatic Ni-Cu-(PGE) systems, when they should float quite rapidly (Fig. 13).

10.2. Survival time

A critical issue regarding the ability of xenophases to play a role in ore formation is their survival time.

10.2.1. Sulfide xenomelts

The survival time of sulfide xenomelts depends on the solubility of sulfide, which varies with temperature, pressure, and magma

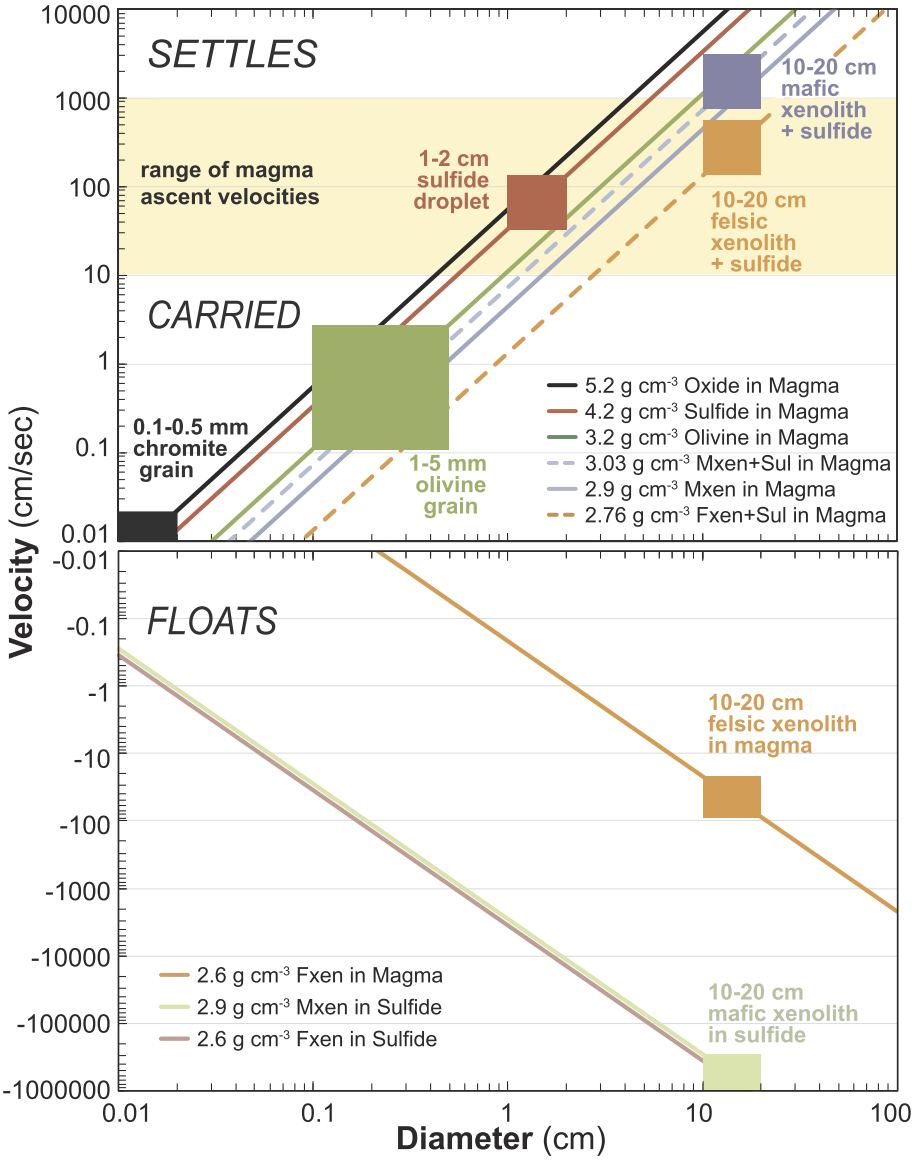

Fig. 13. Maximum settling velocities (estimated using Stokes Law) for chromite, sulfide melt, olivine, mafic xenoliths, mafic xenoliths with 10% sulfide melt, felsic xenoliths, and felsic xenoliths with 10% sulfide melt compared to typical magma ascent velocities (100–1000 cm s^{-1}). Boxes show settling rates for common grain/droplet/xenolith sizes. Magma density assumed to be 2.7 g cm^{-3} and magma viscosity assumed to be 100 g cm^{-1} s^{-1}.

composition. Decreasing pressure will increase solubility, decreasing temperature will decrease solubility, and contamination often decreases sulfide solubility (e.g., Haughton et al., 1974; Shima and Naldrett, 1975; Wendlandt, 1982; Mavrogenes and O'Neill, 1999). However, because the solubility of sulfide in silicate magmas is so low, these effects are minor in high-sulfide Ni-Cu-PGE systems. Only at high magma:sulfide ratios in dynamic systems being replenished by magmas that are undersaturated in sulfide – more likely in komatiitic magmas than in basaltic magmas – will significant amounts of sulfide xenomelts be consumed (Lesher and Burnham, 2001; see also Kerr and Leitch, 2005).

10.2.2. Silicate xenomelts

The survival time of silicate xenomelts can be expected to be relatively short, as they are normally miscible in the silicate magma. In many deposits (e.g., Kambalda, Noril'sk, Raglan, Silver Swan) they are preserved at or near the base of the massive ore horizon, but represent the last material to be melted. At Kambalda – the only clear example – do they appear to have been preserved in flanking sheet-flow facies, where flow was likely less turbulent, not in channel-flow facies, where flow was likely more turbulent.

10.2.3. Xenoliths

Xenoliths may be partly or completely consumed by a magma through reaction, devolatilization, melting, and/or dissolution (e.g., Tsuchiyama, 1986). Devolatilization and melting may occur within the xenolith, so are therefore faster and more efficient, but reaction and dissolution only occur along the margins, so are inherently slower and less efficient (see Robertson et al., 2015). Considering mainly melting, the survival time of xenoliths will depend on several factors (e.g., Bowen, 1922; McLeod and Sparks, 1998):

1) Temperature, viscosity, and density of the magma
2) Initial temperature, mineralogical composition, texture, and density of the xenolith
3) Viscosity and density of any melt/partial melt (mush) layer
4) Solubilities of the various components in the magma
5) Fluid dynamic regime (laminar vs. transitional vs. turbulent)

Xenoliths are less likely to be preserved in hotter, lower viscosity komatiitic magmas than in cooler more viscous basaltic and picritic magmas, and in more dynamic (more turbulent) systems (or parts of systems) than in less dynamic (less turbulent) systems. Mafic lithologies are more refractory, but can melt more rapidly than silicic compositions

because their lower melt viscosities result in thinner melt/mush layers and higher heat fluxes (McLeod and Sparks, 1998). Water-saturated lithologies can melt faster, because of lower melting temperatures and lower melt viscosities. Xenoliths of common continental crustal lithologies in common magmas have been predicted to melt at rates of the order of 2 mm h^{-1} ~ 5 cm d^{-1}, and xenoliths of hot lower continental crustal granulites in basaltic magma have been predicted to melt at rates of the order of 17 mm h^{-1} ~ 40 cm d^{-1} (McLeod and Sparks, 1998). Depending on the relative ascent/settling velocities of the xenoliths, the survival time of all but very large blocks can be relatively short, explaining why many mineralized bodies contain few if any xenoliths and why, where present, they are much more common along the margins rather than the interiors of magmatic bodies.

This means that the abundances and densities of xenoliths may change with time, depending on the temperature and fluid dynamic regime of the lava/magma, the mechanical state of the protolith, and time. For example, during waxing phases of lava/magma flow, xenoliths may be more rapidly incorporated and assimilated, whereas during waning phases of lava/magma flow, xenoliths may be less rapidly incorporated and assimilated. Further, as a xenolith is incorporated it will, depending on its composition and texture, modally or incongruently melt (see e.g., Ripley and Alawi, 1988; Samalens et al., 2017), which will normally (albeit not always) increase its density but which may also reduce its size and/or induce fragmentation. Felsic xenoliths incorporated at depth will progressively become metamorphosed, partially melt, and normally (but again not always) become denser. Mafic melts generally increase in density as they crystallize plagioclase and accumulate Fe-Ti. Assimilation of felsic components, which typically have partial molar volumes less than the corresponding solid phases of inclusions, will partially offset this increase, but in the dynamic systems that form magmatic Ni-Cu-(PGE) deposits it will be the presence of xenoliths that will have the greatest influence on bulk magma density.

Xenoliths may also be infiltrated by the host magma. Many ultramafic inclusions in the Contact Sublayer at Sudbury, even those that are clearly exotic, have highly incompatible and moderately incompatible lithophile element geochemical patterns that are more-or-less identical to the host magma (e.g., Lightfoot et al., 1997). This has been used as evidence for a cognate origin, but where the inclusions are clearly not cognate (e.g., because they contain textures associated with shock metamorphism and/or abundant phlogopite, which is only a minor phase in the rest of the rocks) it must record cryptic melt infiltration that overwhelms the abundance of trace elements in the mesocumulate-adcumulate inclusions. However, this will rarely affect the physical properties, as infiltration of significant amounts of melt normally results in disaggregation.

10.2.4. Xenocrysts

Xenocrysts may also react, devolatilize, melt, and/or dissolve with the magma. Whether residual/cognate xenocrysts are preserved/generated or not depends on the composition of the magma, the composition of the precursor xenolith, and the dynamics of the system (e.g., Bowen, 1922; McLeod and Sparks, 1998). If the xenolith is less mafic than the xenolith, it may dissolve or partially melt – congruently or incongruently – and will be less likely to leave residual xenocrysts or to generate cognate xenocrysts. If the xenolith is more mafic than the magma, it may react with the magma to and will be more likely to produce residual or cognate xenocrysts.

10.3. Implications for the transport of sulfide melts

Sulfide melts can be physically transported in lava/magmas in several ways:

1) Dilute (≤10–15%) suspensions of small (< 1 cm) droplets (e.g., Lesher and Groves, 1986; de Bremond d'Ars et al., 2001) where coalescence is inhibited by the small sizes of the droplets and/or breakup during turbulent flow (Robertson et al., 2016). Coarser droplets will be more susceptible to coalescence and more likely settle depending on magma ascent rates (Fig. 13). The solubility of S at sulfide saturation increases with decreasing pressure (e.g., Wendlandt, 1982; Mavrogenes and O'Neill, 1999), resulting in dissolution of sulfide, but dissolution is slow relative to magma ascent rates (Robertson et al., 2015) and the change – of the order of 0.04% S (~0.1% sulfide) between 30 kb and the surface – is only significant when considering physical transport of very small concentrations of sulfides.
2) Greater abundances and/or coarser droplets in suspension with xenoliths/xenocrysts/xenovolatiles:
   a) If the xenoliths/xenocrysts are less dense than the magma this will facilitate upward transport of sulfides (Fig. 13), however, if the xenoliths/xenocrysts are more dense than the magma, they will facilitate downward transport (Fig. 13). Piña et al. (2006) suggested that the high density of the sulfide-rich magma helped entrain the inclusions at Aguablanca, but the reverse is also likely true: that the inclusions facilitated upward transport of dense sulfide.
   b) Sulfide melts can wet olivine under high fO_2 conditions (e.g., Rose and Brenan, 2001) and to a lesser degree pyroxene, but at most localities sulfides do not appear to wet silicate inclusions. Normally only where sulfide is the continuous phase – as in semi-massive ores - does sulfide wet silicate inclusions. This is because the presence of silicate melt inhibits wetting by sulfide (see Mungall and Su, 2005), which suggests that it is unlikely that silicate xenoliths can transport attached sulfide melts unless they are composed primarily of olivine and unless the fO_2 is high.
   c) Xenovolatiles are always much less dense that the magma, so vesicles will always enhance upward transport and/or retard downward transport (Eckstrand and Williamson, 1985; Ripley et al., 1998; Mungall et al., 2015; Fig. 14).
3) Magmas containing greater than ~8% chromite or ~15% sulfide will be denser than surrounding crust (Fig. 14) and will be more susceptible to "flooding", where the continuous phase changes from less dense silicate magma containing sulfide droplets to denser sulfide magma containing silicate droplets and/or inclusions, resulting in countercurrent (backwards/downwards) flow of the sulfide-rich phase (Fig. 15). Thus, it does not seem likely that chromite or sulfides can be transported as very dense semi-massive to massive slugs, unless emplaced very rapidly through seismic pumping (e.g., Maier et al., 2016) or graben collapse, but even in those situations it

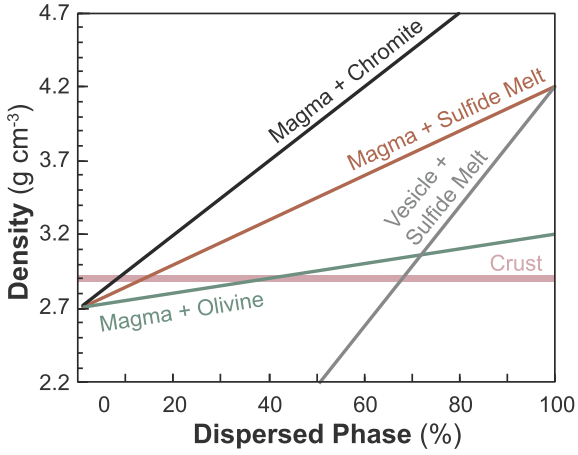

Fig. 14. A (top): Plot of bulk magma density vs sulfide and chromite content. For a bulk crustal density of 2.9 g cm^{-3} the maximum sulfide content for dispersed buoyant magma transport is ~13% and that the maximum sulfide content for dispersed buoyant magma transport is ~13%. B (bottom): Plot of bulk magma density vs vesicle and sulfide content. For a magma density of 2.7 g cm^{-3} the maximum sulfide content for transport by vesicles is ~53%.

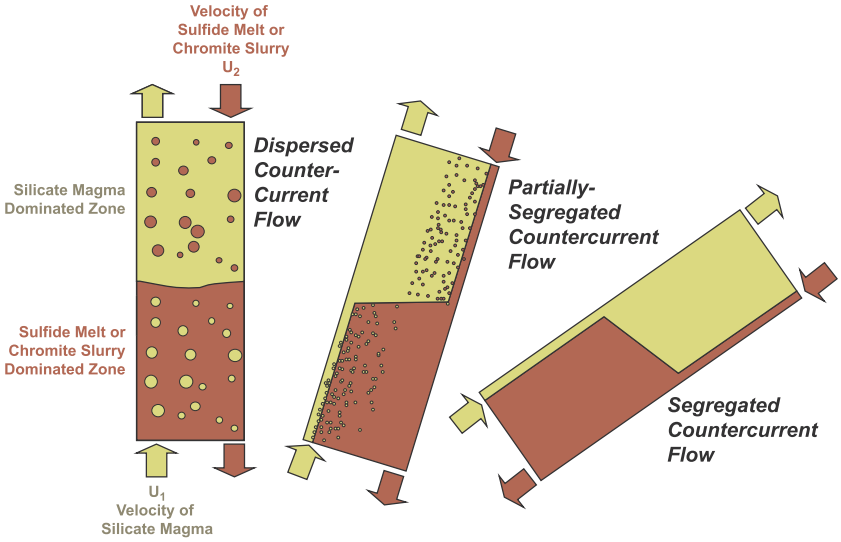

Fig. 15. Flow patterns in vertical, subvertical, and inclined countercurrent flow (modified from Ullmann et al., 2003).

has not been demonstrated that the physics permits dense sulfide melts to be transported upward for significant distances. Tectonic pumping (e.g., Papunen, 2003) is likely too slow. These models require further testing.

The residence time of inclusions also influences sulfide transport:

1) Deeper crustal xenoliths, which might have aided transport by reducing the bulk densities of mafic-ultramafic magmas, may not survive and might only be detected afterwards by their influence on the composition of the magma as it dissolves the inclusions. Because the densities of silicate melts are normally $\sim 0.1–0.2\ g\ cm^{-3}$ less than corresponding solids, melting xenoliths will further decrease the bulk density of the magma, but this will be normally be offset by the crystallization that normally accompanies assimilation (e.g., Bowen, 1922; DePaolo, 1981).
2) Felsic xenoliths incorporated at depth may initially facilitate upward sulfide transport by reducing the bulk density of the lava/magma, but over time as they become metamorphosed, partially melt, and become denser, this will retard upward transport and facilitate sulfide deposition or downward transport.
3) Local xenoliths, which also might have contributed S, may be preserved as their residence time will be shorter, but may not have much influence on sulfide transport except to help retard sulfide (if less dense than the magma) or to increase (if more dense than the magma) settling of sulfide.

Although it is theoretically possible for small amounts of sulfides to be "drawn up" after having accumulated at the base of an intrusion (see discussion by Saumur et al., 2015a), the absence of Ni-Cu-(PGE) mineralization in lavas above mineralized sills (e.g., Noril'sk-Talnakh, Duluth) except where there is evidence of incorporation of S at that level (e.g., Raglan), provides strong support for the concept that significant amounts of sulfides cannot be transported upwards. Indeed, there is an increasing appreciation that sulfides are more likely to flow downward than upward in magmatic systems (e.g., Lesher, 2009; Arndt et al., 2013; Lesher, 2013a,b; Barnes et al., 2016; Saumur et al., 2015b; Hughes et al., 2016).

10.4. Ore localization

Most massive to semi-massive Ni-Cu-PGE and some massive to semi-massive Cr mineralization is localized within dynamic magmatic systems (e.g., Lesher et al., 1984; Lesher, 1989; Naldrett, 2004, 2011; Arndt et al., 2005; Barnes and Lightfoot, 2005; Ripley and Li, 2011; Barnes et al., 2016; Lesher et al., submitted), and more specifically within particular parts of those systems (Fig. 16):

1) Embayments beneath lava channels and channelized sheet flows, of which there are two types:
   a) Linear embayments in which lava/magma and sulfides flowed along their length (e.g., Alexo: Houlé and Lesher, 2011; most parts of Kambalda: e.g., Gresham and Loftus-Hills, 1981; Lesher, 1989)
   b) Elliptical to irregular embayments in which sulfides accumulated (e.g., some parts of Kambalda: Lesher, 1989; Langmuir: Green and Naldrett, 1981; Raglan: Lesher, 2007: Sudbury contact ores: Lightfoot, 2016)
2) Widened parts of dikes and step-overs in dikes (e.g., Sudbury offset ores: e.g., Farrow and Lightfoot, 2002; Lightfoot, 2016; parts of Voisey's Bay: Evans-Lamswood et al., 2000; Lightfoot and Evans-Lamswood, 2015; Saumur et al., 2015)
3) Throats of magma conduits (e.g., Eagle: Ding et al., 2010; Jingbulake: Yang et al., 2012, Tamarack: Taranovic et al., 2016; other parts of Voisey's Bay: Evans-Lamswood et al., 2000)
4) Subhorizontal parts of dike-chonolith and dike-sill complexes (e.g., Noril'sk: e.g., Naldrett, 2004; South Raglan: Mungall, 2007; Thompson: e.g., Layton-Matthews et al., 2010)

Although there were undoubtedly secondary topographic features that influenced the localization of mineralization along the lengths of linear embayments, many Kambalda ore shoots appear to have originally extended over significant distances, so the localization appears to have been controlled primarily by gravitational flow segregation rather than abrupt fluid dynamic changes.

The other ore-localizing features have been interpreted to represent places where fluid dynamic conditions abruptly changed, facilitating deposition of dense sulfide, chromite, and/or xenoliths. In these cases, the ore-localizing features are interpreted to have operated as reverse venturis (nozzles) in various orientations (subvertical in Fig. 17), where conservation of mass dictates:

$$Q = p_e\ u_e\ A_e = p_c\ u_c\ A_c = p_x\ u_x\ A_x$$

where $\boldsymbol{Q}$ is mass flow rate, $\boldsymbol{p_e}$, $\boldsymbol{p_c}$, and $\boldsymbol{p_x}$ are bulk densities, $\boldsymbol{u_e}$, $\boldsymbol{u_c}$, and $\boldsymbol{u_x}$ are velocities, and $\boldsymbol{u_e}$, $\boldsymbol{u_c}$, and $\boldsymbol{u_x}$ are cross-sectional areas for a narrow entry feeder $\boldsymbol{e}$, a wider ore-localizing conduit/chamber $\boldsymbol{c}$, and a narrow exit feeder $\boldsymbol{x}$.

Continuity requires that at constant $\boldsymbol{Q}$, increasing $\boldsymbol{A_c}$ (i.e., unconstricting flow) leads to a decrease in $\boldsymbol{u_c}$. Flow velocities are higher in the entry and exit feeders, lower in a narrow chamber, and much lower

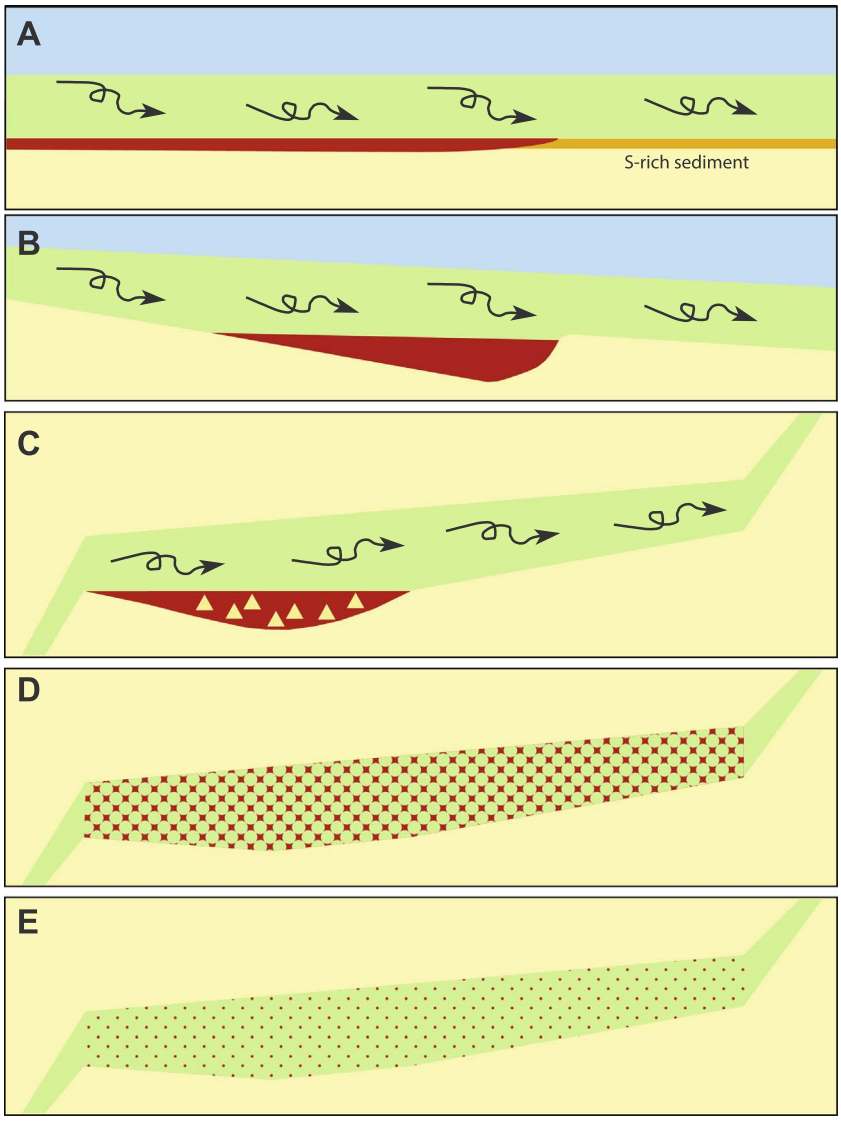

Fig. 16. Schematic representations of ore-localizing mechanisms for Ni-Cu-PGE and Cr deposits. Yellow: footwall rocks, blue: seawater or hanging wall rocks, green: magma. A: Longitudinal section through a dynamic (flow-through) submarine lava channel or channelized sill/chonolith eroding a S-rich substrate and generating sulfide xenomelt. B: Longitudinal section through a dynamic submarine lava channel or channelized sill/chonolith containing a second-order embayment that collects sulfide xenomelt. C: Cross/longitudinal section through a dynamic channelized sill/chonolith containing a second-order embayment with sulfide xenomelt ± inclusions concentrated near the entry point. D: Cross/longitudinal section through a dynamic channelized sill/chonolith containing a "filter bed" of olivine cumulates ± inclusions that have collected and accumulated fine disseminated sulfides. E: Cross/longitudinal section through a dynamic channelized sill/chonolith containing olivine-(sulfide) "cotectic" cumulates.

in a wider chamber (Fig. 17A-B), favouring deposition of denser components (sulfide melt, chromite, and/or inclusions) (Fig. 17C). This may become a self-perpetuating process as the magma continues to stope the wall rocks in the chamber more rapidly than the wall rocks of the entry and exit dikes/sills. A consequence of such a process is that deposition of dense sulfide melt, chromite, and/or xenoliths within the conduit/chamber will be accompanied by a reduction in $\boldsymbol{p_x}$ and therefore with all else equal a corresponding increase in $\boldsymbol{u_x}$.

Many models (e.g., Mungall and Su, 2005; Chung and Mungall, 2009; Barnes et al., 2017a,b) emphasize the effects of surface tension and gravitationally-driven migration/percolation of sulfide melt. These are undoubtedly important in modifying disseminated, patchy disseminated, net, and patchy-net textures after deposition, but accumulation of sulfide melt in dynamic systems was more likely dominated by channelized advective, often turbulent flow (Fig. 16A-C), intergranular dynamic connectivity (à la Reynolds, 2017) in the case of xenocryst/phenocryst/primocryst filter beds (Fig. 16D), and the potential for countercurrent flow of silicate magma and sulfide melt and inclusions in the case of inclusion-rich ores.

Indeed, within the context of the constraints on S sources and the complexities of transporting dense sulfides/oxides noted above, it seems likely that the sulfides/oxides in many systems flowed/settled downward and were trapped in the same throats/transitions that have been proposed to have trapped upward-transported sulfides (Fig. 17C-D). For example, Ding et al. (2012) showed that the mass-independent S isotopic data at Eagle required a deeper source and therefore upward transport, most of the data summarized in Fig. 5 and elsewhere suggest local sources and therefore lateral – if any – transport, and Holwell et al. (2012) and Hughes et al. (2016) showed that mass-dependent S isotopic data in West Greenland macrodikes and olivine-rich plugs on Rum required a shallower source and therefore downward transport. More detailed studies of this type are obviously required, but within the context of this discussion it is clear that sulfides/oxides are just as likely to have formed via downward transport than by upward transport, that both may have operated in the same deposit at different times, as magma fluxes waxed and waned, and therefore that any of the models in Fig. 17C-E are capable of localizing Ni-Cu-PGE sulfides or chromite.

11. Conclusions

1) Xenoliths, xenocrysts, xenomelts, and xenovolatiles play active and sometimes critical roles in ore genesis and are valuable exploration indicators.
2) Sulfide xenomelts are the most common product of the ore-formation process in Ni-Cu-PGE deposits. The metal tenors and isotopic compositions of the ores and other components in the system depend on the initial composition of the sulfide xenomelt, the composition of the silicate magma, the sulfide/silicate partition

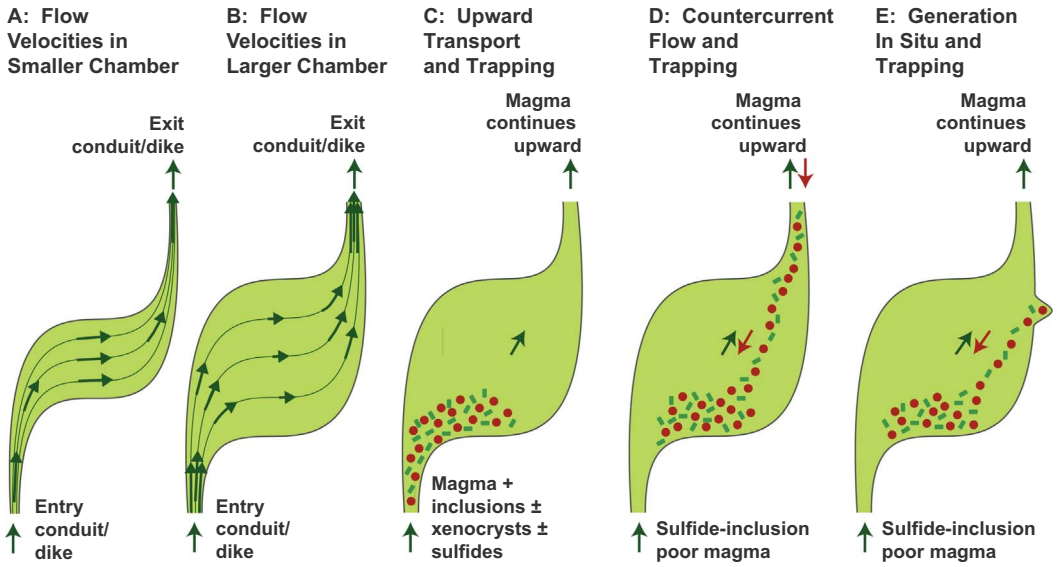

Fig. 17. Sulfide collection mechanisms accompanying velocity changes in a magma channel/chonolith/dike segment/magma chamber. A and B: Schematic mass flux/density/velocity model for magma entering through a narrower conduit/dike, passing through a slightly wider (A) and much wider (B) channel/chonolith/dike chamber/magma chamber, and exiting through a narrower conduit/dike. Lengths of arrows are proportional to velocity and distances between flow lines are inversely proportional to velocity. C: Traditional model in which an upward-ascending magma containing inclusions ± xenocrysts ± sulfide enters from below and deposits them near the entry point because of the reduction in magma velocity. D and E: Alternative models in which inclusions ± xenocrysts ± sulfide are generated above the level of the chamber (D) or within the chamber (E), settle downwards countercurrent to magma flow, and are deposited near the entry point, prevented from setting further by the higher velocity of flow in the entry conduit/dike.

coefficient, and the magma:sulfide mass ratio.

3) Silicate xenomelts other than those in emulsion ores are rare, but potentially quite valuable mineralization indicators, as they will be depleted in chalcophile metals and are direct evidence of the formation of a Ni-Cu-PGE-enriched sulfide xenomelt.
4) Xenoliths contribute S and sometimes metals in most Ni-Cu-PGE deposits and strongly influence the bulk density and viscosity of the magma and therefore sulfide transport. Although xenoliths that are lighter than the magma may facilitate upward transport by decreasing bulk density, they normally become denser as they are metamorphosed and partially melted. They can be diagnostic mineralization indicators and provide important constraints on sulfide/oxide sources.
5) Xenocrysts *appear* to be less commonly preserved, but some chromite deposits may represent accumulations of fine Fe ± Ti oxide xenocrysts that have been converted to chromite during transport in Cr-rich magmas.
6) Xenovolatiles are common where lavas/magmas have incorporated unconsolidated sediments and/or volcanic rocks, and because of their very low density have the greatest potential to enhance the upward ascent of dense Fe-Ni-Cu sulfide melts.
7) Most magmatic Ni-Cu-PGE deposits and some Cr deposits are localized in dynamic magmatic systems, particularly in embayments/jogs/throats that represent changes in fluid dynamic regime and which have been interpreted to represent traps for collecting upward-transported sulfides/oxides/xenoliths, but which may equally represent traps for collecting downward-transported sulfides/oxides/xenoliths.

Acknowledgements

This research has been supported at various stages by grants from the US National Science Foundation, the Natural Sciences and Engineering Council of Canada Discovery/CRD/IRC programs, the Ontario Geological Survey and Geological Survey of Canada, BHP Billiton Ltd., Cliffs Natural Resources Inc., Falconbridge/Xstrata/Glencore Ltd., Inco/Vale Ltd., Noront Ltd., Outokumpu Ltd., and Western Mining Corporation. I am very grateful to many colleagues for discussions on these topics, especially Nick Arndt, Sarah-Jane Barnes, Steve Barnes, Marcus Burnham, Ian Campbell, Paul Golightly, David Groves, Michel Houlé, Jon Hronsky, Reid Keays, Ed Pattison, and Ed Ripley, to Steve Barnes and an anonymous reviewer for helpful comments on the original manuscript, and to Franco Pirajno and Marco Fiorentini for editorial assistance.

Appendix A. Supplementary data

Supplementary data associated with this article can be found, in the online version, at http://dx.doi.org/10.1016/j.oregeorev.2017.08.008.

References

Arndt, N.T., Lesher, C.M., Czamanske, G.K., 2005, Mantle-derived magmas and magmatic Ni-Cu-(PGE) deposits, 100th Anniversary Volume, Society of Economic Geologists, 5–23.

Arndt, N.T., Barnes, S.J., Robertson, J., Lesher, C.M., Cruden, S., 2013. Downward injection of sulfide slurries: their role in the formation of Ni sulfide deposits, Goldschmidt Conference, Florence. Mineral. Mag. 77 (5), 618.

Bavinton, O.A., 1981. The nature of sulfidic sediments at Kambalda and their broad relationships with associated ultramafic rocks and nickel ores. Econ. Geol. 76, 1606–1628.

Barnes, S.-J., Lightfoot, P.C., 2005. Formation of magmatic nickel sulfide ore deposits and processes affecting their copper and platinum group element contents. 100th Anniversary Volume, Society of Economic Geologists, 179–214.

Barnes, S.J., Heggie, G.J., Fiorentini, M.L., 2013. Spatial variation in platinum group element concentrations in ore-bearing komatiite at the Long-Victor deposit, Kambalda Dome, Western Australia: enlarging the footprint of nickel sulfide orebodies. Econ. Geol. 108, 913–933.

Barnes, S.J., Cruden, A.R., Arndt, N., Saumur, B.M., 2016. The mineral system approach applied to magmatic Ni-Cu-PGE sulphide deposits. Ore Geol. Rev. 76, 296–316.

Barnes, S.J., Mungall, J.E., Le Vaillant, M., Godel, B., Lesher, C.M., Holwell, D., Lightfoot, P.C., Krivolutskaya, N., Wei, B., 2017a. Sulfide-silicate textures in magmatic Ni-Cu-PGE sulfide ore deposits: 1. Disseminated and net-textured ores. Am. Mineral. 102 (3), 473–507.

Barnes, S.J., Le Vaillant, M., Lightfoot, P.C., 2017b. Textural development in sulfide-matrix ore breccias in the Voisey's Bay Ni-Cu-Co deposit, Labrador, Canada. Ore Geol. Rev this volume.

Bekker, A., Barley, M.E., Fiorentini, M.L., Rouxel, O.J., Rumble, D., Beresford, S.W., 2009. Atmospheric sulfur in Archean komatiite-hosted nickel deposits. Science 326, 1086–1089.

Bleeker, W., 1990. Evolution of the Thompson Nickel Belt and its Nickel Deposits, Manitoba. PhD thesis, University of New Brunswick, Fredericton, 400.

Bowen, N.L., 1922. The behavior of inclusions in igneous magmas. J. Geol. 30 (S6), 513–570.

Brügmann, G.E., Naldrett, A.J., Asif, M., Lightfoot, P.C., Gorbachev, N.S., Fedorenko, V.A., 1993. Siderophile and chalcophile metals as tracers of the evolution of the Siberian Trap in the Noril'sk region, Russia. Geochim. Cosmochim. Acta 57, 2001–2018.

Campbell, I.H., Barnes, S.J., 1984. A model for the geochemistry of the platinum group elements in magmatic sulphide deposits. Can. Mineral. 22, 151–160.

Campbell, I.H., Naldrett, A.J., 1979. The influence of silicate:sulfide ratios on the geochemistry of magmatic sulphides. Econ. Geol. 74, 1503–1506.

Carson, H.J.E., Lesher, C.M., Houlé, M.G., 2015. Geochemistry and Petrogenesis of the Black Thor Intrusive Complex, McFaulds Lake Greenstone Belt, Ontario, Canada. In: D.E. Ames, M.G. Houlé (Ed.), Targeted Geoscience Initiative 4, Canadian Nickel-Copper-Platinum Group Elements-Chromium Ore Systems—Fertility, Pathfinders, New and Revised Models, Geological Survey of Canada, Open File 7856, 89–101.

Chai, G., Naldrett, A.J., 1992. Characteristics of Ni-Cu-PGE mineralization and genesis of the Jinchuan deposit, northwest China. Econ. Geol. 87, 1475–1495.

Choudhuri, A., Iyer, S.S., Krouse, H.R., 1997. Sulfur isotopes in komatiite-hosted Ni-Cu sulfide deposits from the Morro do Ferro greenstone belt, southeastern Brazil. Int. Geol. Rev. 39 (3), 230–238.

Chung, H.-Y., Mungall, J.E., 2009. Physical constraints on the migration of immiscible fluids through partially molten silicates, with special reference to magmatic sulfide ores. Earth Planet. Sci. Lett. 286, 14–22.

Cowden, A., Donaldson, M.J., Naldrett, A.J., Campbell, I.H., 1986. Platinum-group elements and gold in the komatiite-hosted Fe–Ni–Cu sulfide deposits at Kambalda, Western Australia. Econ. Geol. 81, 1226–1235.

de Bremond d'Ars, J., Arndt, N.T., Hallot, E., 2001. Analog experimental insights into the formation of magmatic sulfide deposits. Earth Planet. Sci. Lett. 186, 371–381.

DePaolo, D.J., 1981. Trace element and isotopic effects of combined wallrock assimilation and fractional crystallization. Earth Planet. Sci. Lett. 53, 189–202.

Ding, X., Li, C., Ripley, E.M., Rossell, D., Kamo, S., 2010. The Eagle and East Eagle sulfide ore-bearing mafic-ultramafic intrusions in the Midcontinent Rift System, upper Michigan: geochronology and petrologic evolution. Geochem. Geophys. Geosyst. 11 (3). http://dx.doi.org/10.1029/2009GC002546.

Ding, X., Ripley, E.M., Shirey, S.B., Li, C., 2012. Os, Nd, O and S isotope constraints on country rock contamination in the conduit related Eagle Cu-Ni-(PGE) deposit, Midcontinent Rift System, upper Michigan. Geochim. Cosmochim. Acta 89, 10–30.

Donnelly, T.H., Lambert, I.B., Oehler, D.Z., Hallberg, J.A., Hudson, D.R., Smith, J.W., Bavinton, O.A., Golding, L., 1978. A reconnaissance study of stable isotopes ratios in Archaean rocks from the Yilgarn Block, Western Australia. Geol. Soc. Australia J. 24, 409–420.

Dowling, S.E., Barnes, S.J., Hill, R.E.T., Hicks, J.D., 2004. Komatiites and nickel sulfide ores of the Black Swan area, Yilgarn Craton, Western Australia. 2: Geology and genesis of the orebodies. Miner. Deposita 39, 707–728.

Eckstrand, O.R., Williamson, B.L., 1985. Vesicles in the Dundonald komatiites. Program and Abstracts, Geological Association of Canada—Mineralogical Association of Canada Annual Meeting, Abstract Volume 10, A-16.

Evans, D.M., Cowden, A., Barratt, R.M., 1989. Deformation and thermal erosion at the Foster nickel deposit, Kambalda-St. Ives, Western Australia. In: Proceedings of the Fifth Magmatic Sulphide Field Conference, Harare, Zimbabwe. Institution of Mining and Metallurgy, London.

Evans-Lamswood, D.M., Butt, D.P., Jackson, R.S., Lee, D.V., Muggridge, M.G., Wheeler, R.I., Wilton, D.H.C., 2000. Physical Controls Associated with the Distribution of Sulfides in the Voisey's Bay Ni-Cu-Co deposit, Labrador. Econ. Geol. 95, 749–769.

Farhangi, N., Lesher, C.M., Houlé, M.G., 2013, Project Unit 13-002. Mineralogy, Geochemistry and Petrogenesis of Nickel-Copper-Platinum Group Element Mineralization in the Black Thor Intrusive Complex, McFaulds Lake Greenstone Belt, Ontario; in Summary of Field Work and Other Activities, Ontario Geological Survey, Open File Report 6290, 55.1–55.8.

Farrow, C.E.G., Lightfoot, P.C., 2002. Sudbury PGE revisited: toward an integrated model. In: L. Cabri (Ed.), The Geology, Geochemistry, Mineralogy, and Mineral Beneficiation of the Platinum-Group Elements, Canadian Institute of Mining, Metallurgy and Petroleum, Special Volume 54, 273–297.

Farrow, C.E.G., Watkinson, D.H., 1997. Geochemical evolution of the epidote zone, Fraser mine, Sudbury, Ontario: Ni-Cu-PGE remobilization by saline fluids. Explor. Min. Geol. 5 (1), 17–31.

Fiorentini, M., Bekker, A., Rouxel, O., Wing, B.A., Maier, W., Rumble, D., 2012a. Multiple sulfur and iron isotope composition of magmatic Ni-Cu-(PGE) sulfide Mineralization from Eastern Botswana. Econ. Geol. 107, 105–116.

Fiorentini, M., Beresford, S., Barley, M., Duuring, P., Bekker, A., Rosengren, N., Cas, R., Hronsky, J., 2012b. District to camp controls on the genesis of komatiite-hosted nickel sulfide deposits, Agnew-Wiluna Greenstone Belt, Western Australia: insights from the multiple sulfur isotopes. Econ. Geol. 107, 781–796.

Frost, K.M., Groves, D.I., 1989a. Magmatic contacts between immiscible sulfide and komatiite melts; implications for genesis of Kambalda sulfide ores. Econ. Geol. 84, 1697–1704.

Frost, K.M., Groves, D.I., 1989b. Ocellar units at Kambalda: Evidence for sediment assimilation by komatiite lavas. In: Prendergast, M.D., Jones, M.J. (Eds.), Magmatic Sulfides – Zimbabwe Volume, Proceedings of the Fifth Magmatic Sulfide Field Conference, Harare, Zimbabwe. Institution of Mining Metallurgy, London, pp. 207–214.

Green, A.H., Naldrett, A.J., 1981. The Langmuir volcanic peridotite-associated nickel deposits: Canadian equivalents of the Western Australian occurrences. Econ. Geol. 76, 1503–1523.

Gresham, J.J., Loftus-Hills, G.D., 1981. The geology of the Kambalda nickel field, Western Australia. Econ. Geol. 76, 1373–1416.

Grinenko, L.I., 1985. Sources of sulfur of the nickeliferous and barren gabbro-dolerite intrusions of the northwestern Siberian platform. Int. Geol. Rev. 27, 695–708.

Groves, D.I., Korkiakoski, E.A., McNaughton, N.J., Lesher, C.M., Cowden, A., 1986. Field evidence for thermal erosion by komatiites at Kambalda, Western Australia and the genesis of nickel ores. Nature 319, 136–139.

Haughton, D.R., Roeder, P.L., Skinner, B.J., 1974. Solubility of sulfur in mafic magmas. Econ. Geol. 69, 451–467.

Hiebert, R.S., Bekker, A., Wing, B.A., Rouxel, O.J., 2013. The role of paragneiss assimilation in the origin of the Voisey's Bay Ni-Cu sulfide deposit, Labrador: multiple S and Fe isotope evidence. Econ. Geol. 108, 1459–1469.

Hiebert, R.S., Bekker, A., Houlé, M.G., Wing, B.A., Rouxel, O.J., 2016. Tracing sources of crustal contamination using multiple S and Fe isotopes in the Hart komatiite-associated Ni–Cu–PGE sulfide deposit, Abitibi greenstone belt, Ontario, Canada. Miner. Deposita 51, 919–935.

Holwell, D.A., Abraham-James, T., Keays, R.R., Boyce, A.J., 2012. The nature and genesis of marginal Cu-PGE-Au sulphide mineralisation in Paleogene Macrodykes of the Kangerlussuaq region, East Greenland. Mineral. Deposita 47 (1–2), 3–21.

Holwell, D.A., Keays, R.R., Firth, E.A., Findlay, J., 2014. Geochemistry and mineralogy of platinum group element mineralization in the River Valley Intrusion, Ontario, Canada: a model for early-stage sulfur saturation and multistage emplacement and the implications for "contact-type" Ni-Cu-PGE sulfide mineralization. Econ. Geol. 109, 689–712.

Houlé, M.G., Lesher, C.M., 2011. Komatiite-associated Ni-Cu-(PGE) mineralization in the Abitibi Greenstone Belt, Ontario. Rev. Econ. Geol. 17, 89–121.

Houlé, M.G., Lesher, C.M., Davis, P.C., 2012. Thermomechanical erosion and genesis of komatiite-associated Ni-Cu-(PGE) mineralization at the Alexo Mine, Abitibi Greenstone Belt, Ontario. Mineral. Deposita 47 (1–2), 105–128.

Hughes, H.S.R., McDonald, I., Boyce, A.J., Holwell, D.A., Kerr, A.C., 2016. Sulphide sinking in magma conduits: evidence from mafic-ultramafic plugs on rum and the wider North Atlantic Igneous Province. J. Petrol. 57 (2), 383–416.

Huppert, H.E., Sparks, R.S.J., Turner, J.S., Arndt, N.T., 1984. Emplacement and cooling of komatiite lavas. Nature 309, 19–22.

Ivanov, B.A., Deutsch, A., 1999. Sudbury impact event: cratering mechanics and thermal history. Geol. Soc. Am. Spec. Pap. 339, 389–397.

Jugo, P.J., Luth, R.W., Richards, J.P., 2005. An experimental study of the sulfur content in basaltic melts saturated with immiscible sulfide or sulfate liquids at 1,300 C and 1.0 GPa. J. Petrol. 46, 783–798.

Karykowski, B.T., Polito, P.A., Maier, W.D., Gutzmer, J., 2015. Origin of Cu-Ni-PGE mineralization at the Manchego Prospect, West Musgrave Province, Western Australia. Econ. Geol. 110 (8), 2063–2085.

Keays, R.R., Lightfoot, P.C., 2004. Formation of Ni–Cu–platinum group element sulfide mineralization in the Sudbury impact melt sheet. Mineral. Petrol. 82, 217–258.

Keays, R.R., Lightfoot, P.C., 2010. Crustal sulfur is required to form magmatic Ni–Cu sulfide deposits: evidence from chalcophile element signatures of Siberian and Deccan Trap basalts. Miner. Deposita 45, 241–257.

Kerr, A., Leitch, A.M., 2005. Self-destructive sulfide segregation systems and the formation of high-grade magmatic ore deposits. Econ. Geol. 100, 311–332.

Kinnaird, J.A., Hutchinson, D., Schurmann, L., Nex, P.A.M., De Lange, R., 2005. Petrology and mineralisation of the Southern Platreef, northern limb of the Bushveld Complex, South Africa. Mineral. Deposita 40, 576–597.

Kullerud, G., Yund, R.A., Moh, G., 1969. Phase relations in the Fe-Ni-S, Cu-Fe-S, and Cu-Ni-S systems. Econ. Geol. Monogr. 4, 323–343.

Labidi, J., Cartigny, P., Birck, J.L., Assayag, N., Bourrand, J.J., 2012. Determination of multiple sulfur isotopes in glasses: a reappraisal of the MORB $\delta^{34}S$. Chem. Geol. 334, 189–198.

Layton-Matthews, D.M., Lesher, C.M., Burnham, O.M., Hulbert, L., Peck, D.C., Golightly, J.P., Keays, R.R., 2010. Exploration for Ni-Cu-(PGE) deposits in the Thompson nickel belt, Manitoba. Soc. Econ. Geol. Spec. 15, 513–538.

Le Vaillant, M., Barnes, S.J., Mungall, J.E., Mungall, E., 2017. Role of de-gassing of the Noril'sk nickel deposits in the Permo-Triassic mass extinction event. Proc. Natl. Acad. Sci. 114 (10), 2485–2490.

Lesher, C.M., 1989. Komatiite-associated nickel sulfide deposits. In: Whitney, J.A., Naldrett, A.J. (Eds.), Ore Deposition Associated with Magmas, Reviews in Economic Geology 4. Economic Geology Publishing Company, El Paso, pp. 45–101.

Lesher, C.M., 2007. Ni-Cu-(PGE) Deposits in the Raglan Area, Cape Smith Belt, New Québec. In: W.D. Goodfellow (Editor), Mineral Resources of Canada: A Synthesis of Major Deposit-types, District Metallogeny, the Evolution of Geological Provinces, and Exploration Methods, Geological Survey of Canada and Mineral Deposits Division of the Geological Association of Canada Special Publication 5, 351–386.

Lesher, C.M., 2009, Generation, transport, and collection of Fe-Ni-Cu sulfide melts. In: Proceedings of the Xi'an International Ni-Cu-(Pt) Symposium, Northwestern Geology 42, 6–9.

Lesher, C.M., 2013a. The roles of local incorporation, in-situ segregation, and physical transport in the genesis of magmatic sulfide and oxide deposits, GAC-MAC Annual Meeting, Winnipeg, Abstract Volume, 128–129.

Lesher, C.M., 2013b. Physical transport and localization of magmatic Fe-Ni-Cu sulfide melts. In: Conference Proceedings, SEG 2013: Geoscience for Discovery, Whistler BC, Society of Economic Geologists, abstract (p18) and poster (P1.12), ISBN 978-1-629492-66-7.

Lesher, C.M., 2013c, Catastrophic sulfide saturation and genesis of Ni-Cu-PGE mineralization in the Sudbury Igneous Complex. In: Proceedings of the 12th Biennial SGA Meeting, v3, Uppsala, Sweden, 1040–1043.

Lesher, C.M., Arndt, N.T., 1995. Trace element and Nd isotope geochemistry, petrogenesis, and volcanic evolution of contaminated komatiites at Kambalda, Western Australia. Lithos 34, 127–157.

Lesher, C.M., Barnes, S.J., 2009. Komatiite-associated Ni-Cu-(PGE) deposits. In: Li, C., Ripley, E.M. (Eds.), Magmatic Ni-Cu-PGE Deposits: Genetic Models and Exploration. Geological Publishing House of China, pp. 27–101.

Lesher, C.M., Burnham, O.M., 2001. Multicomponent elemental and isotopic mixing in Ni-Cu-(PGE) ores at Kambalda, Western Australia. Can. Mineral. 39, 421–446.
Lesher, C.M., Campbell, I.H., 1993. Geochemical and fluid dynamic modeling of compositional variations in Archean komatiite-hosted nickel sulfide ores in Western Australia. Econ. Geol. 88, 804–816.
Lesher, C.M., Groves, D.I., 1986. Controls on the formation of komatiite-associated nickel–copper sulfide deposits. In: Friedrich, G.H., Genkin, A.D., Naldrett, A.J. (Eds.), Geology and Metallogeny of Copper Deposits. Springer, pp. 43–62.
Lesher, C.M., Keays, R.R., 1984. Metamorphically and hydrothermally mobilized Fe-Ni-Cu sulphides at Kambalda, Western Australia. In: Buchanan, D.L., Jones, M.J. (Eds.), Sulphide Deposits in Mafic and Ultramafic Rocks. Institution of Mining and Metallurgy, London, pp. 62–69.
Lesher, C.M., Keays, R.R., 2002. Komatiite-associated Ni-Cu-(PGE) deposits: Mineralogy, geochemistry, and genesis. In: Cabri, L.J. (Ed.), The Geology, Geochemistry, Mineralogy, and Mineral Beneficiation of the Platinum-Group Elements. Special vol. 54. Canadian Institute of Mining, Metallurgy, and Petroleum, pp. 579–617.
Lesher, C.M., Stone, W.E., 1996. Exploration geochemistry of komatiites. In: Wyman, D. (Ed.), Igneous Trace Element Geochemistry: Applications for Massive Sulphide Exploration. Geological Association of Canada, Short Course Notes 12, 153–204.
Lesher, C.M., Lee, R.F., Groves, D.I., Bickle, M.J., Donaldson, M.J., 1981. Geochemistry of komatiites from Kambalda, Western Australia: I. Chalcophile element depletion - a consequence of sulfide liquid separation from komatiitic magmas. Econ. Geol. 76, 1714–1728.
Lesher, C.M., Arndt, N.T., Groves, D.I., 1984. Genesis of komatiite-associated nickel sulphide deposits at Kambalda, Western Australia: a distal volcanic model. In: Buchanan, D.L., Jones, M.J. (Eds.), Sulphide Deposits in Mafic and Ultramafic Rocks. Institution of Mining and Metallurgy, London, pp. 70–80.
Lesher, C.M., Barnes, S.-J., Gillies, S.L., and Ripley, E.M., 1999. Ni-Cu-(PGE) sulphides in the Raglan Block, in Lesher CM (Editor), Komatiitic Peridotite-Hosted Fe-Ni-Cu-(PGE) Sulphide Deposits in the Raglan Area, Cape Smith Belt, New Québec. Guidebook Series 2, Mineral Exploration Research Centre, Laurentian University, Sudbury: 177–184.
Lesher, C.M., Burnham, O.M., Keays, R.R., Barnes, S.J., Hulbert, L., 2001. Trace-element geochemistry and petrogenesis of barren and ore-associated komatiites. Can. Mineral. 39, 673–696.
Lesher, C.M., Carson, H.J.E., Metsaranta, R.T., Houlé MG, 2014. Genesis of chromite deposits by partial melting, physical transport, and dynamic upgrading of silicate-magnetite facies iron formation. In: 12th International Platinum Symposium, Yekaterinburg, Russia, Extended Abstract Volume, 36–38.
Lesher, C.M., Carson, H.J.E., Houlé, M.G., 2016. Genesis of chromite by dynamic upgrading of xenocrystic Fe ± Ti oxide, 35th International Geological Congress, Cape Town, South Africa. Extended Abstract Volume, 3892.
Lesher, C.M., Carson, H.J.E., Houlé, M.G., submitted. Genesis of chromite by dynamic upgrading of xenocrystic Fe ± Ti oxide, Geology.
Li, C., Naldrett, A.J., 2000. Melting reactions of gneissic inclusions with enclosing magma at Voisey's Bay, Labrador, Canada; implications with respect to ore genesis. Econ. Geol. 95, 801–814.
Li, C., Ripley, E.M., 2005. Empirical equations to predict the sulfur content of mafic magmas at sulfide saturation and applications to magmatic sulfide deposits. Miner. Deposita 40, 218–230.
Lightfoot, P.C., 2016. Nickel Sulfide Ores and Impact Melts: Origin of the Sudbury Igneous Complex. Elsevier 680p.
Lightfoot, P.C., Evans-Lamswood, D.M., 2015. Structural controls on the primary distribution of mafic–ultramafic intrusions containing Ni–Cu–Co–(PGE) sulfide mineralization in the roots of large igneous provinces. Ore Geol. Rev. 64, 354–386.
Lightfoot, P.C., Keays, R.R., Morrison, G.G., Bite, A., Farrell, K.P., 1997. Geologic and geochemical relationships between the contact Sublayer, inclusions, and the Main Mass of the Sudbury Igneous Complex—a case study of the Whistle Mine embayment. Econ. Geol. 92, 647–673.
Lightfoot, P.C., Keays, R.R., Evans-Lamswood, D., Wheeler, R., 2012. S saturation history of Nain plutonic suite mafic intrusions: origin of the Voisey's Bay Ni–Cu–Co sulfide deposit, Labrador, Canada. Miner. Deposita 47, 23–50.
Maier, W.D., Smithies, R.H., Spaggiari, C.V., Barnes, S.J., Kirkland, C.L., Yang, S., Lahaye, Y., Kiddie, O., MacRae, C., 2016. Petrogenesis and Ni–Cu sulphide potential of mafic–ultramafic rocks in the Mesoproterozoic Fraser Zone within the Albany-Fraser Orogen, Western Australia. Precambrian Res. 281, 27–46.
Mainwaring, P.R., Naldrett, A.J., 1977. Country rock assimilation and genesis of Cu-Ni sulfides in the Water Hen intrusion, Duluth Complex, Minnesota. Econ. Geol. 72, 1269–1284.
Mariga, J., Ripley, E.M., Li, C., 2006. Petrologic evolution of gneissic xenoliths in the Voisey's Bay Intrusion, Labrador, Canada: mineralogy, reactions, partial melting, and mechanisms of mass transfer. Geochem. Geophys. Geosyst. 7 (5), 25.
Mavrogenes, J.A., O'Neill, H.S.C., 1999. The relative effects of pressure, temperature and oxygen fugacity on the solubility of sulfide in mafic magmas. Geochim. Cosmochim. Acta 63, 1173–1180.
McCormick, K.A., Fedorowich, J.S., McDonald, A.M., James, R.S., 2002. A textural, mineralogical, and statistical study of the footwall breccia within the Strathcona embayment of the Sudbury Structure. Econ. Geol. 97, 125–143.
McNamara, G.S., Lesher, C.M., Kamber, B.S., 2017. New feldspar lead isotope and trace element evidence from the Sudbury Igneous Complex indicate a complex origin of associated Ni-Cu-PGE mineralization involving underlying country rocks. Econ. Geol. 112 (3), 569–590.
McLeod, P., Sparks, R.S.J., 1998. The dynamics of xenolith assimilation. Contrib. Miner. Petrol. 132, 21–33.
Menard, T., Lesher, C.M., Stowell, H.H., Price, D.P., Pickell, J.R., Hulbert, L., 1996. Geology, genesis, and metamorphic history of the Namew Lake Fe-Ni-Cu-PGE deposit, Manitoba. Econ. Geol. 91, 1394–1413.
Mungall, J.E., 2007. Crustal contamination of picritic magmas during transport through dikes: the expo intrusive suite, Cape Smith Fold Belt, New Quebec. J. Petrol. 48, 1021–1039.
Mungall, J.E., Su, S., 2005. Interfacial tension between magmatic sulfide and silicate liquids: constraints on kinetics of sulfide liquation and sulfide migration through silicate rocks. Earth Planet. Sci. Lett. 234, 135–149.
Mungall, J.E., Harvey, J.D., Balch, S.J., Azar, B., Atkinson, J., Hamilton, M.A., 2010. Eagle's Nest: A magmatic Ni-sulfide deposit in the James Bay Lowlands, Ontario. Society of Economic Geologists, Special Publication, Canada 15: 539–557.
Mungall, J.E., Brenan, J.M., Godel, B., Barnes, S.J., Gaillard, F., 2015. Transport of metals and sulphur in magmas by flotation of sulphide melt on vapour bubbles. Nat. Geosci. 8, 216–219.
Naldrett, A.J., 1966. The role of sulphurization in the genesis of iron-nickel sulphide deposits of the Porcupine District, Ontario. Can. Inst. Mining Metal. Trans. 69, 147–155.
Naldrett, A.J., 2004. Magmatic Sulfide Deposits: Geology, Geochemistry and Exploration. Springerpp. 727.
Naldrett, A.J., 2011. Fundamentals of magmatic sulfide deposits. In: Li, C., Ripley, E.M. (Ed.), Magmatic Ni-Cu and PGE deposits: Geology, Geochemistry, and Genesis: Reviews in Economic Geology 17, 1–50.
Naldrett, A.J., Hewins, R.H., Dressler, B.O., Rao, B.V., 1984. The contact sublayer of the Sudbury igneous complex. In: Pye, E.G., Naldrett, A.J., Giblin, P.E. (Ed.), The Geology and Ore Deposits of the Sudbury Structure. Ontario Geological Survey Special Publication 1, 253–274.
Nelles, E., 2012. Genesis of Cu-PPGE-rich veins and Au-Pd-Pt-Ni-Te-rich disseminated footwall mineralization in the Sudbury Igneous Complex, unpublished MSc thesis, Laurentian University, Sudbury, 77 pp.
Nelles, E., Lesher, C.M., in revision. Genesis of Cu-PGE-rich Footwall-Type Mineralization in the Morrison Deposit, Sudbury. Economic Geology.
Papunen, H., 2003. Ni-Cu sulfide deposits in mafic-ultramafic orogenic intrusions: examples from the Svecofennian areas, Finland. In: Elipoulos et al. (Eds.), Mineral Exploration and Sustainable Development, Millpress, Rotterdam, 551–554.
Pattison, E., 1979. The Sudbury sublayer. Can. Mineral. 17, 257–274.
Peck, D.C., Keays, R.R., James, R.S., Chubb, P.T., Reeves, S.J., 2001. Controls on the formation of contact-type platinum-group element mineralization in the East Bull Lake intrusion. Econ. Geol. 96, 559–581.
Perring, C.S., Barnes, S.J., Hill, R.E.T., 1995. The physical volcanology of komatiite sequences from Forrestania, Southern Cross Province, Western Australia. Lithos 34, 189–207.
Petford, N., 2009. Which effective viscosity? Mineral. Mag. 73 (2), 167–191.
Piña, R., Lunar, R., Ortega, L., Gervilla, F., Alapieti, T., Martinez, C., 2006. Petrology and geochemistry of mafic–ultramafic fragments from the Aguablanca Ni–Cu Ore Breccia, Southwest Spain. Econ. Geol. 101, 865–881.
Prendergast, M.D., 2001. Komatiite-hosted Hunters Road nickel deposit, central Zimbabwe: physical volcanology and sulfide genesis. Aust. J. Earth Sci. 48, 681–694.
Prevec, S.A., Lightfoot, P.C., Keays, R.R., 2000. Evolution of the sublayer of the Sudbury Igneous Complex: geochemical, Sm–Nd isotopic and petrologic evidence. Lithos 51, 271–292.
Raskevicius, T., 2013. Reaction between magmatic sulfide melts and wall rocks in the Sudbury Igneous Complex. unpublished BSc Hons thesis Laurentian University, Sudbury, pp. 27.
Reynolds, C.A., Menkea, H., Andrew, M., Blunt, M.J., Krevora, S., 2017. Dynamic fluid connectivity during steady-state multiphase flow in a sandstone. Proc. Natl. Acad. Sci. www.pnas.org/cgi/doi/10.1073/pnas.1702834114 [Early Access].
Ripley, E.M., 1981. Sulfur isotopic studies of the Dunka Road Cu-Ni deposit, Duluth Complex, Minnesota. Econ. Geol. 76, 610–620.
Ripley, E.M., 1986. Application of stable isotopic studies to problems of magmatic sulfide ore genesis with special reference to the Duluth Complex, Minnesota. In: Friedrich, G., Genkin, A.D., Naldrett, A.J., Ridge, J.D., Sillitoe, R.H., Vokes, F.M. (Eds.), Geology and Metallogeny of Copper Deposits. Springer-Verlag, Berlin, pp. 25–42.
Ripley, E.M., Alawi, J.A., 1988. Petrogenesis of pelitic xenoliths at the Babbitt Cu-Ni deposit, Duluth Complex, Minnesota, U.S.A. Lithos 21 (2), 143–159.
Ripley, E.M., Li, C., 2003. Sulfur isotope exchange and metal enrichment in the formation of magmatic Cu-Ni-(PGE) deposits. Econ. Geol. 98, 635–641.
Ripley, E.M., Li, C., 2011. A review of conduit related Ni–Cu–(PGE) sulfide mineralization at the Voisey's Bay deposit, Labrador, and the Eagle deposit, northern Michigan. In: Li, C., Ripley, E.M. (Eds.), Magmatic Ni–Cu and PGE Deposits: Geology, Geochemistry and Genesis, Reviews in Economic Geology 17. Society of Economic Geologists, Denver, Colorado, pp. 181–198.
Ripley, E.M., Li, C., 2013. Sulfide saturation in mafic magmas: Is external sulfur required for magmatic Ni-Cu-(PGE) ore genesis? Econ. Geol. 108, 45–58.
Ripley, E.M., Severson, M.J., Hauk, S.A., 1998. Evidence for Sulfide and Fe-Ti-P-Rich Liquid Immiscibility in the Duluth Complex Minnesota. Econ. Geol. 93, 1052–1062.
Ripley, E.M., Park, Y.R., Li, C., Naldrett, A.J., 1999. Sulfur and oxygen isotopic evidence of country rock contamination in the Voisey's Bay Ni-Cu-Co deposit, Labrador, Canada. Lithos 47, 53–68.
Ripley, E.M., Li, C., Shin, D., 2002. Paragneiss assimilation in the genesis of magmatic Ni-Cu-Co sulfide mineralization at Voisey's Bay, Labrador: $\delta^{34}S$, $\delta^{13}C$, and Se/S evidence. Econ. Geol. 97, 1307–1318.
Ripley, E.M., Lightfoot, P.C., Stifter, E.C., Underwood, B., Taranovic, V., Dunlop III, M., Donoghue, K.A., 2015. Heterogeneity of S isotope compositions recorded in the Sudbury igneous complex, Canada: significance to formation of Ni-Cu sulfide ores and the host rocks. Econ. Geol. 110, 1125–1135.
Robertson, J., Ripley, E.M., Barnes, S.J., Li, C., 2015. Sulfur liberation from country rocks and incorporation in mafic magmas. Econ. Geol. 110, 1111–1123.

Robertson, J.C., Barnes, S.J., Le Vaillant, M., 2015. Dynamics of magmatic sulphide droplets during transport in silicate melts and implications for magmatic sulphide ore formation. J. Petrol. 56, 2445–2472.
Rose, L.A., Brenan, J.M., 2001. Wetting properties of Fe-Ni-Co-Cu-O-S melts against olivine: implications for sulfide melt mobility. Econ. Geol. 96, 145–157.
Sakai, H., Marais, D., Ueda, A., Moore, J., 1984. Concentrations and isotope ratios of carbon, nitrogen and sulfur in ocean-floor basalts. Geochim. Cosmochim. Acta 48 (12), 2433–2441.
Samalens, N., Barnes, S.-J., Sawyer, E.J., 2017. The role of black shales as a source of sulfur and semimetals in magmatic nickel copper deposits: example from the Partridge River Intrusion, Duluth Complex, Minnesota, USA. Ore Geol. Rev. 81, 173–187.
Saumur, B.M., Cruden, A.R., Boutelier, D., 2015a. Sulfide liquid entrainment by silicate magma: implications for the dynamics and petrogenesis of magmatic sulfide deposits. J. Petrol. 56 (12), 473–2490.
Saumur, B.M., Cruden, A.R., Evans-Lamswood, D.M., Lightfoot, P.C., 2015b. Wall-Rock Structural Controls on the Genesis of the Voisey's Bay Intrusion and its Ni-Cu-Co Magmatic Sulfide Mineralization (Labrador, Canada). Econ. Geol. 110, 691–711.
Seat, Z., Beresford, S.W., Grguric, B.A., Waugh, R.S., Hronsky, J.M.A., Gee, M.A.M., Groves, D.I., Mathison, C.I., 2007. Architecture and emplacement of the Nebo-Babel gabbronorite-hosted magmatic Ni-Cu-PGE sulphide deposit, West Musgrave, Western Australia. Mineral. Deposita XX, XXX-XXX.
Seat, Z., Beresford, S.W., Grguric, B.A., Gee, M.A.M., Grassineau, N.V., 2009. Reevaluation of the role of external sulfur addition in the genesis of Ni-Cu-PGE Deposits, Evidence from the Nebo-Babel Ni-Cu-PGE Deposit, West Musgrave, Western Australia. Econ. Geol. 104, 521–538.
Seccombe, P.K., Groves, D.I., Binns, R.A., Smith, J.W., 1978. A sulfur isotopic study to test a genetic model for Fe-Ni sulphide mineralization at Mt Windarra, Western Australia. In: B.W. Robinson (Ed.), Stable isotopes in the earth sciences. New Zealand Department of Scientific and Industrial Research, Wellingston, DSIR Bull 220, 187–200.
Seccombe, P.K., Groves, D.I., Marston, R.J., Barrett, F.M., 1981. Sulfide paragenesis and sulfur mobility in Fe-Ni-Cu sulfide ores at Lunnon and Juan Main Shoots, Kambalda: textural and sulfur isotopic evidence. Econ. Geol. 76, 1675–1685.
Shaw, H.R., 1972. Viscosities of magmatic silicate liquids: an empirical method of prediction. Am. J. Sci. 272 (870), 893.
Shima, H., Naldrett, A.J., 1975. Solubility of sulfur in an ultramafic melt and the relevance of the system Fe-S-O. Econ. Geol. 70, 960–967.
Spath, C.S. III, 2017. Geology and Genesis of Hybridized Ultramafic Rocks in the Black Label Hybrid Zone of the Black Thor Intrusive Complex, McFaulds Lake Greenstone Belt, Ontario, Canada, unpublished MSc thesis, Laurentian University, 102 pp.
Spath, C.S. III, Lesher, C.M, Houlé, M.G, 2015. Hybridized ultramafic rocks in the Black Label hybrid zone of the Black Thor intrusive complex, McFaulds Lake greenstone belt, Ontario. In: D.E. Ames and M.G. Houlé (Ed.), Targeted Geoscience Initiative 4: Canadian Nickel-Copper-Platinum Group Elements-Chromium Ore Systems—Fertility, Pathfinders, New and Revised Models, Geological Survey of Canada, Open File 7856, 105–114.
Sproule, R.A., Sutcliffe, R., Tracanelli, H., Lesher, C.M., 2008. Palaeoproterozoic Ni-Cu-PGE mineralization in the Shakespeare Intrusion: a new style of Nipissing gabbro-hosted mineralization. Inst. Min. Metal. 116 (4), 188–200.
Staude, S., Barnes, S.J., Le Vaillant, M., 2016. Evidence of lateral thermomechanical erosion of basalt by Fe-Ni-Cu sulfide melt at Kambalda, Western Australia. Geology 44, 1047–1050.
Staude, S., Le Vaillant, M., Barnes, S.J., 2017. Thermomechanical excavation of ore-hosting embayments beneath komatiite lava channels: textural evidence from the Moran deposit, Kambalda, Western Australia. Ore Geol. Rev this volume.
Taranovic, V., Ripley, E.M., Li, C., Rossell, D., 2016. Chalcophile element (Ni, Cu, PGE, and Au) variations in the Tamarack magmatic sulfide deposit in the Midcontinent Rift System: implications for dynamic ore-forming processes. Miner. Deposita 51, 937–951.
Thériault, R.D., Barnes, S.-J., 1998. Compositional variations in Cu-Ni-PGE sulfides of the Dunka Road deposit, Duluth Complex, Minnesota: the importance of combined assimilation and magmatic processes. Can. Mineral. 36, 869–886.
Tsujimura, T., Kitakaze, A., 2004. New phase relations in the Cu-Fe-S system at 800 C; constraints of fractional crystallization of a sulfide liquid. Neues Jahrbuch für Mineralogie - Monatshefte 2004, 433–444.
Tsuchiyama, A., 1986. Melting and dissolution kinetics: application to partial melting and dissolution of xenoliths. J. Geophys. Res. 91 (B9), 9395–9406.
Tyson, R.M., Chang, L.L.Y., 1984. The petrology and sulfide mineralization of the Partridge River troctolite, Duluth Complex, Minnesota. Can. Mineral. 22, 23–38.
Ullmann, A., Zamir, M., Ludmer, Z., Brauner, N., 2003. Stratified laminar countercurrent flow of two liquid phases in inclined tubes. Int. J. Multiph. Flow 29, 1583–1604.
Wang, Y., Lesher, C.M., Lightfoot, P.C., 2016. Shock metamorphic features of olivine, orthopyroxene, amphibole, and plagioclase in phlogopite-bearing ultramafic-mafic inclusions in Contact Sublayer, Sudbury Igneous Complex, PDAC Annual Meeting, Toronto.
Wang, Y., Lesher, C.M., Lightfoot, P.C., Pattison, E.F., Golightly, J.P., 2016. Shock metamorphic features of olivine, orthopyroxene, amphibole, and plagioclase in phlogopite-bearing ultramafic-mafic inclusions in Contact Sublayer, Sudbury Igneous Complex, 35th International Geological Congress, Capetown, South Africa, Abstract Volume, 5802.
Wendlandt, R.F., 1982. Sulfide saturation of basalt and andesite melts at high pressures and temperatures. Am. Mineral. 67, 877–885.
Williams, D.A., Kerr, R.C., Lesher, C.M., 1998. Emplacement and erosion by Archean komatiite lava flows: revisited. J. Geophys. Res. 103 (B11), 27533–27549.
Williams, D.A., Kerr, R.C., Lesher, C.M., Barnes, S.J., 2002. Analytical/numerical modeling of komatiite lava emplacement and thermal erosion at Perseverance, Western Australia. J. Volcanol. Geoth. Res. 110, 27–55.
Yang, S.-H., Zhou, M.-F., Lightfoot, P.C., Malpas, J., Qu, W.-J., Zhou, J.-B., Kong, D.-Y., 2012. Selective crustal contamination and decoupling of lithophile and chalcophile element isotopes in sulfide-bearing mafic intrusions: an example from the Jingbulake Intrusion, Xinjiang, NW China. Chem. Geol. 302–303, 106–118.